

SATELLITE CELLS AND MYOTONIC DYSTROPHY TYPE 1 (DM1)

**CHARACTERIZATION OF SATELLITE CELLS AND ASSOCIATED MYOGENIC
DEFECTS IN DM1 WITH AEROBIC TRAINING**

By KATHERINE MANTA, BSc Life Sciences

A Thesis Submitted to the School of Graduate Studies in Partial Fulfilment of the Requirements
for the Degree Master of Science - Medical Sciences

MASTER OF SCIENCE (2021)
Medical Sciences

McMaster University
Hamilton, Ontario

TITLE: Characterization of satellite cells and associated myogenic defects
in myotonic dystrophy type 1(DM1) with aerobic training

AUTHOR: Katherine Manta, B.Sc. Kin (McMaster University)

SUPERVISOR: Dr. Mark A. Tarnopolsky

PAGES: 71

Lay Abstract

Myotonic dystrophy type 1 (DM1) is the most common muscular dystrophy in adults worldwide affecting 1:8000 individuals, with certain areas in northeastern Quebec having a higher prevalence of 1:600 individuals. DM1 is caused by an autosomal dominant genetic mutation that leads to muscle weakness, respiratory insufficiency, cataracts and cardiac conduction block, ultimately resulting in poor quality of life and shortened lifespan. Preliminary evidence suggests that the maintenance of muscle health can greatly improve quality of life and life-span of these individuals, making an in-depth research focus on this therapeutic intervention extremely important. Optimal muscle health is maintained by the functionality of muscle stem cells, that aid in muscle repair and facilitate adaptations in muscle following exercise interventions. These cells are shown to be dys- or non-functional in various muscular dystrophies which coincide with the observation of poor muscle health. Therefore, the aim of this study was to examine the number and functionality of muscle stem cells, and physiological factors of muscle health in DM1. In addition, we also aimed to explore whether exercise has therapeutic potential to alleviate poor muscle quality in DM1. In general, we found that DM1 patients have a higher proportion of muscle stem cells; however, they are inherently dysfunctional but did respond to exercise. Consistent with the latter observation, we found poor muscle quality metrics in DM1 patients, with aerobic training leading to improvements in muscle health. Altogether, our results provide in-depth analysis that underscores muscle dysfunction observed in DM1 and the benefits of exercise interventions.

Abstract

Myotonic dystrophy type 1 (DM1) is an autosomal dominant and progressive neuromuscular disorder caused by the CTG trinucleotide repeat expansion in the 3' untranslated region of the DMPK gene. Clinical manifestations include extensive atrophy of skeletal muscle (SkM) concomitant with muscle weakness, that develops in a distal to proximal fashion. Central to muscle plasticity is the satellite cell (SC), a muscle specific stem cell that, upon activation, facilitates muscle repair and regeneration. To date, SCs have yet to be elucidated in DM1; therefore, the aim of the present study was to extensively characterize the PAX7⁺ SC population, along with other indices of muscle quality in SkM. DM1 patients (6 women, 5 men) performed stationary cycling 3 times per week for 12wks, with biopsies taken from the *Vastus lateralis* pre- (PRE) and post-endurance exercise intervention (POST). Age-matched, healthy controls (CTRL) were used for comparison of baseline measures. Type 1 and 2 myofiber-specific PAX7⁺ cells were significantly greater in DM1 patients (PRE), in comparison to CTRL (2.24- and 1.84-fold, respectively), with type 2 SC content further increasing following training ($p < 0.05$). In addition, protein expression of myogenic regulatory factors PAX7 and myogenin were significantly higher in DM1 compared to CTRL, with no training effects observed. Both immunohistochemical and immunoblotting analysis showed that activated MYOD⁺/PAX7⁺ cells did not significantly differ in DM1 vs. CTRL. FISH- IF analysis of CUG repeats show that 30% of SCs in DM1 were positive for these inclusions. Muscle capillarization was significantly lower in type 2 fibers in DM1 vs CTRL, which was fully rescued with training ($p < 0.05$). At baseline, DM1 muscle showed the presence of *de novo* and fat infiltrated fibres, as well as fibrosis, that were relatively non-existent in the CTRL. *In vitro* results show patient-derived myoblasts exhibit a proliferation defect. Furthermore, myoblasts showed impairments in both glycolysis and mitochondrial respiration, with the latter being completely

normalized to CTRL in myotubes. Our novel findings display an increased, albeit non-functional, SC pool in DM1 SkM indicated by disturbances in the myogenic program and overall poor muscle quality. We show that both SCs and SkM remain responsive to exercise training, suggesting therapeutic potential. We also suggest that mitochondrial dysfunction may underpin these impairments in the myogenic program.

Acknowledgements

I would like to thank Dr. Tarnopolsky for taking me on as a Master student and a fourth-year volunteer, enabling me to explore my scientific interests. Thank you for your support, patience, and guidance throughout the years especially during the pivot of my thesis project due to the COVID-19 pandemic. Thank you to Dr. Nederveen, for your day-to-day mentorship and ongoing support. You constantly provided me with new challenges to grow as a researcher and instilled both a work ethic in me and a passion for scientific exploration that inspired me to pursue research in the future. Thank you for believing in me and embarking on the pursuit of various “moonshot experiments”. I would like to thank Dr. Morrison and Dr. Hawke for your ongoing support as my committee through uncertain times of the pandemic and enabling me to transition to a new project seamlessly. Thank you Dr. Ljubicic for taking the time to serve as my external committee. Thank you to Linda May and Bart Hettinga for all your work making sure the lab stays afloat. Finally, I would like to thank Donald Xhuti, Andrew Mikhail and Matthew Fuda.

Table of Contents

Lay Abstract	4
Abstract	5
Acknowledgements	7
List of Figures and Tables	10
<i>Figure 1. DM1 muscle exhibits increased satellite cell pool, and fusion markers</i>	<i>10</i>
<i>Figure 2. SCs in DM1 possess CUG nuclear foci accumulation</i>	<i>10</i>
<i>Figure 3. DM1 muscle has markers of poor muscle quality</i>	<i>10</i>
<i>Figure 4. DM1 patient myoblasts have a proliferation defect</i>	<i>10</i>
<i>Figure 5. DM1 myoblasts display decreased respiratory capacity and glycolysis, oxygen consumption normalized in myotubes</i>	<i>10</i>
Review of The Literature	11
<i>List of Acronyms</i>	<i>11</i>
<i>Introduction to DM1</i>	<i>13</i>
<i>Cause of DM1</i>	<i>13</i>
<i>Classification of DM1</i>	<i>14</i>
<i>Clinical Presentations & Manifestations</i>	<i>14</i>
<i>Pathophysiology of the Disease</i>	<i>16</i>
<i>Toxic Gain and Loss of Function of MBNL and CUGBP1</i>	<i>16</i>
<i>AMPK and DM1</i>	<i>17</i>
<i>Mitochondria and DM1</i>	<i>19</i>
<i>Introduction to Satellite Cells</i>	<i>20</i>
<i>Myogenic Program</i>	<i>21</i>
<i>Satellite Cells and DM1</i>	<i>21</i>
<i>Failure of Proliferation in DM1 and Autophagy</i>	<i>23</i>
<i>Differentiation Defect in DM1</i>	<i>24</i>
<i>RNA Toxicity and SCs in DM1</i>	<i>26</i>
<i>DM1 and Premature Senescence</i>	<i>27</i>
<i>Satellite Cells and Mitochondria</i>	<i>28</i>
<i>Satellite Cell and Mitochondria- Implications for Muscular Dystrophies</i>	<i>30</i>
Thesis Purpose, Objectives, Hypothesis	31
Introduction	35
<i>Ethical approval</i>	<i>37</i>
<i>Participants</i>	<i>37</i>

<i>Training Intervention</i>	38
<i>Muscle Biopsies</i>	38
<i>Immunohistochemical Staining</i>	39
<i>Histochemical Staining</i>	41
<i>Protein Extraction and Immunoblotting in vivo</i>	42
<i>Fluorescent in Situ Hybridization (FISH)</i>	43
<i>Cell Culture</i>	44
<i>Proliferation Protocol</i>	44
<i>Differentiation Protocol</i>	45
<i>Immunofluorescence</i>	45
<i>Immunoblotting and Protein Extraction in vitro</i>	46
<i>Statistical Analysis</i>	47
Results	48
<i>Figure 1. DM1 muscle exhibits increased satellite cell pool, and fusion markers</i>	49
<i>Figure 2. SCs in DM1 possess CUG nuclear foci accumulation</i>	51
<i>Figure 3. DM1 muscle has markers of poor muscle quality</i>	53
<i>Figure 4. DM1 patient myoblasts have a proliferation defect</i>	54
<i>Figure 5. DM1 myoblasts display decreased respiratory capacity and glycolysis, oxygen consumption normalized in myotubes</i>	56
Discussion	57
<i>Elevated SC pool in DM1</i>	57
<i>DM1 SCs are responsive to exercise</i>	61
<i>Skeletal muscle ‘quality’ improved after exercise</i>	63
<i>Impaired mitochondrial respiration in DM1 myoblasts, normalization with differentiation</i>	64
Conclusion	67
References	70

List of Figures and Tables

Figures from Literature Review

Figure 1. Metabolic Orchestration of Myogenic Program

Tables from Methods

Table 1. Participant Characteristics and Adherence

Table 2: Antibody information for staining muscle cross sections

Table 3. *In vitro* myoblast characteristics

Table 4. Antibody information for western blotting *in vitro*

Figures from Results

Figure 1. DM1 muscle exhibits increased satellite cell pool, and fusion markers.

Figure 2. SCs in DM1 possess CUG nuclear foci accumulation.

Figure 3. DM1 muscle has markers of poor muscle quality.

Figure 4. DM1 patient myoblasts have a proliferation defect.

Figure 5. DM1 myoblasts display decreased respiratory capacity and glycolysis, oxygen consumption normalized in myotubes.

Figures from Discussion

Figure 1. Summary of Results

Review of The Literature

List of Acronyms

AICAR - 5-aminoimidazole-4-carboxamide 1- β -D-ribofuranoside, Acadesine, N1-(β

D-ribofuranosyl)-5-aminoimidazole-4-carboxamide

AMPK - 5' AMP-activated protein kinase

AKT. - Protein kinase B

BIN-1 - Bridging integrator 1

cDM1 – congenital myotonic dystrophy type 1

CLC1 - muscle-specific chloride channel

C/Fi – capillaries per fibre

CFPE – capillary fibre perimeter exchange

CoQ10 - Coenzyme Q10

CRISPR/Cas9 - Clustered regularly interspaced short palindromic repeats/CRISPR associated protein 9

CSA – cross sectional area

CUGBP1 - CUG binding protein Elav-like family member 1

DM1 - Myotonic Dystrophy Type 1

DMD - Duchenne Muscular Dystrophy

DMPK - dystrophia myotonica protein kinase

DRP1 - Dynamin-1-like protein

ECAR – extracellular acidification rate

ECG - electrocardiogram

eMHC – embryonic myosin heavy chain

ETC – electron transport chain

GSK3b – Glycogen synthase kinase 3 beta

HSA-LR - human skeletal actin, long-repeats

iPSCs – induced pluripotent stem cells

LC3 - Microtubule-associated proteins 1A/1B light chain 3B

MFN1 - Mitofusin-1

MBNL1 - Muscleblind-like protein

mTORC1 - mammalian target of rapamycin complex 1

Mrf4 - Myogenic factor 6

MyoD - myoblast determination protein 1

Myf5 - Myogenic factor 5

OCR – oxygen consumption rate

OPA1 - Mitochondrial dynamin like GTPase OPA1

OXPPOS - Oxidative phosphorylation

Pax7 – pair box like transcription factor 7

PGC1a - PPARg coactivator-1 alpha

Ryr1 - ryanodine receptor 1

ROS - Reactive oxygen species

SC – Satellite cell

SERCA1 - sarco(endo)plasmic reticulum calcium-ATPase 1

TALEN - Transcription activator-like effector nucleases

TNNT3 - troponin T3

ULK1 - Unc-51 like autophagy activating kinase

UTR – untranslated region

Introduction to DM1

Myotonic Dystrophy Type 1 (DM1) or Steinart's Disease is an autosomal dominant multisystemic disorder, primarily affecting skeletal and smooth muscle¹. It is hallmarked by muscle atrophy, degeneration and myotonia due to excessive muscle excitability^{2,3}. DM1 is the most common muscular dystrophy in adults, affecting ~1:8000 individuals worldwide and as high as 1:600 in Saguenay-Lac St. Jean, Quebec, Canada^{1,4}. The variability in prevalence can be accounted for by the colonization that occurred in Quebec during the 17th and 19th centuries by a relatively small group of affected French settlers, leading to the loss of genetic variability and increased prevalence of heritable diseases⁴. This phenomenon is denoted as the founder effect. It is suggested that the prevalence of DM1 is likely an underestimate due to mild cases going undetected. The genetic prevalence of the disease has recently been discovered to be four times higher, at ~1:2000, as determined by screening of the genetic mutation of DM1 in newborn blood samples from 50,000 births that occurred between 2013 and 2014 in New York⁵.

Cause of DM1

The pathology of the disease stems from an autosomal dominant inheritance of the microsatellite trinucleotide CTG repeat expansion in the 3' untranslated region of *DMPK* transcript located on chromosome 19q13⁶. The discovery of the mutation that causes DM1 has led to the ability to diagnose repeats in venous blood samples of DM1 patients, improving diagnostic accuracy, and enabling accurate genetic counseling. The number of repeats is proportional to both the severity of the disease and to the onset^{2,3}. The inheritance of the CTG triplet repeat or

‘expansion’ also exhibits generational anticipations, where both the severity and onset increase in successive generations due to the accumulation instability of the tandem repeat, causing expansion during mitosis^{2,3}. Studies have shown that in successive generations, the mutation can grow an additional ~200 repeats^{7,8}. Anticipation “jumps” of more than 1000 repeats are greater with maternal transmission, accounting for nearly all cDM1 patients^{7,9}. However, paternal inheritance tends to be associated with greater repeat instability and anticipation of the premutation to those observed in classic DM1^{10,11}.

Classification of DM1

Due to the large heterogeneity of the disease, it is categorized into three main subdivisions based on the severity: congenital DM1 (cDM1), classic DM1, and mild DM1^{2,3}. Healthy individuals possess CUG repeats ranging from 5-37, beyond this range is considered pathological^{2,3}. Repeat numbers between 38-49 is considered a premutation allele as these individuals are asymptomatic but risk having children that may have DM1 due to anticipation and allele instability^{2,3}. Possession of 50 to 150 repeats is categorized by late onset, mild DM1 having no change in lifespan.^{2,3} 100 to 1000 CUG repeats is categorized as classic DM1 exhibiting adult onset and a decreased lifespan^{2,3}. A quantification of >1000 repeats is classified as cDM1 and displays an early onset and markedly shortened life-span^{2,3}.

Clinical Presentations & Manifestations

The clinical manifestations of the disorder drastically range from mild cases to lethal cases which is both affected by the age of onset and the number of CUG repeats the individually inherits^{2,3}. Given the wide-ranging nature of DM1, classical adult onset DM1 will be the focus of

the current investigation/thesis. The onset of the classical adult onset form occurs normally around 20 to 30 years of age; however, signs and symptoms may be evident (often in retrospect) in childhood-most often beginning with myotonia².

The hallmark symptoms of DM1 include muscle weakness/atrophy and myotonia (sustained muscular contractions)^{2,3}. Muscular dystrophy in DM1 progresses in a distal to proximal fashion, whereby degeneration of the distal muscles occurs first^{2,3}. Phenotypically, this presents as gait abnormalities (i.e., foot drop), due to preferential atrophy of dorsiflexors and difficulty with hand strength/dexterity due weakness of the finger flexor and intrinsic hand muscles^{2,3}. Facial features include ptosis (i.e., drooping of the eye lids), weak smile and thin face caused by a weakness in facial muscles as all cranial muscles are negatively affected^{2,3}. In advanced cases, DM1 eventually affects the proximal limb muscle leading to wheelchair confinement, the respiratory muscles leading to hypoventilation and the oropharyngeal muscles leading to dysphagia and aspiration; collectively increasing morbidity and reducing life expectancy².

In terms of the effect on cardiac tissue, ~24% DM1 patients will eventually exhibit abnormal cardiac conduction as diagnosed through ECG primarily through a prolonged PR interval and/or QRS duration¹². Cardiac abnormalities are significant as they lead to shorter lifespan due to and sudden death from arrhythmias^{2,3}. Due to dysfunction of smooth muscle DM1 patients have a greater risk for gastrointestinal dysmotility, gallbladder dysfunction and constipation^{2,3}. The diaphragm and intercostal muscles (both skeletal muscle) often show weakness and even myotonia, that collectively can further exacerbate ventilation defects and ultimately play a major role in the lethality of the disease^{2,3}. Indeed, the most common causes of death from DM1 are; acute respiratory and cardiac failure, pneumonia, neoplasms, and cardiovascular disease^{2,3}. Cognitive impairments are evident in some cases of mild and classic DM1 resulting in lower IQ, processing

capabilities, sleep disturbances and the presence of mental health disorders. Cataracts is also present with DM1^{2,3}. Classical DM1 is associated with thyroid dysfunction, calcium irregularities, diabetes mellitus, hyperinsulinism, low vitamin D levels, although levels of severities and clinical significance of these endocrine functions vary between patients¹³. Further, CUG repeats also increases the risk of various cancers (e.g., uterine, testicular, thyroid, prostate, ovary, choroidal, endometrium, colon, brain, pilomatricoma), and this increased risk is not observed in family members that do not have DM1^{2,3}. Taken together, DM1 was a multisystemic disorder which may lend itself to therapies that target several different risk factors and/or tissues.

Pathophysiology of the Disease

The microsatellite cell expansion causes dysfunction at all levels of cell including chromatin function, DNA replication and transcription, mRNA processing, translation and signalling, leading to the multifaceted defects associated with the disorder¹⁴. For the purposes of this review and project, we will be focusing on the main pillar underlying the disorder, RNA toxicity, along with lesser-known metabolic defects associated with the disorder.

Toxic Gain and Loss of Function of MBNL and CUGBP1

The clinical presentation of DM1 likely stems from a toxic RNA gain-of-function, instead of a loss of transcription and/or protein dysfunction. Due to the location of the tandem repeat mutation at the last exon of the transcript, the mutation does not blunt transcription of the *DMPK* gene³. Instead, this leads to the formation of abnormal mRNA structures, possessing a microsatellite expansion^{15,16}. The mutant mRNA aggregates into “hairpin loops” at the end of the *DMPK* transcript which is stabilized by both base pair binding and intramolecular forces¹⁷. This

hairpin structure ultimately leads to the alteration of two major proteins: MBLN and CUGBP1. These repeats are not able to exit the nucleus and reach the cytoplasm leading to hallmark phenotypic “foci”, or retention of mutant mRNA^{15,16}. Ultimately, this suggests that the primary mechanism underlying the disease is the build-up of CUG repeats which in turn, sequesters specific RNA and DNA binding proteins.

MBNL proteins bind to the hairpin structure with high affinity, a collection of proteins widely used for the regulation of splicing, RNA transport and degradation^{18,19}. However, these proteins become sequestered in the nucleus, meaning they are unable to perform their functions in the cytoplasm. Downstream splicing targets of MBNL include; CLC1 channels in muscle accounting for myotonia²⁰, insulin receptors²¹, BIN-1²², dystrophin and L-type calcium channels further contributing to the myopathy in DM1^{23,24}. The mutation also leads to the hyperphosphorylation of CUGBP1, or a toxic gain of function. CUGBP1 is the topic of much of the impairments present in myoblasts, which is discussed in further detail later.

AMPK and DM1

AMPK is the major regulator in cellular energy status by sensing the concentrations of AMP/energy charge and is activated by metabolic stressors that increase the consumption of ATP or inhibits its production²⁵. AMPK restores energy balance by activating a number of downstream targets involved in catabolism, ATP generating pathways, and by inhibiting anabolic pathways²⁵. Using human skeletal actin promoter (HSA^{LR}) mouse models, Brockhoff and colleagues (2017) found a reduction in the phosphorylation status of AMPK in DM1 during starved conditions (a stimulus that induces AMPK activation), while mTORC1 signalling remained activated²⁶. Similarly, research showed that lower AMPK phosphorylation in patient-derived myoblasts,

correlating with lower PGC1a levels, a regulator in mitochondrial biogenesis²⁷. Treatment of mice with acute and chronic dosing of a pharmacological AMPK activator (AICAR) resulted in less myotonia and a partial rescue of chloride channels and nuclear CUG foci dispersion in HSA^{LR} mice^{26,27}. Interestingly, treatment with rapamycin (mTORC1 inhibitor) resulted in improvements in myotonia, force generation without splicing improvements²⁶. Ravel-Chapuis and colleagues (2018) showed similar positive effects with 6 weeks of AICAR administration (AMPK activation) resulted in improvements in muscle histology, including increases in type 2a muscle fibers, improvements in oxidative phosphorylation (OXPHOS)-related protein content, increases in muscle cross-sectional area (CSA) and decreases in central nucleation, which is indicative of ongoing regeneration in a fibre²⁷. In primary myoblasts, AICAR treatments were shown to have a dose dependent positive effect on dispersion of MBNL, decreased activity of CUGBP1 as well as normalization of other proteins involved in the spliceopathy of the disease.²⁷

A well-known potent activator of AMPK is exercise, supporting the notion that this can be beneficial in individuals with DM1. In fact, voluntary wheel running improved alternative splicing *SERCA1*, *RyR1*, *TNNT3* and *CLC1*²⁷. More recently, Manta and colleagues (2019) demonstrated that voluntary wheel running in HSA^{LR} mice resulted in improvements in the myopathy of the disease along with improvements in OXPHOS, and citrate synthase protein levels. Furthermore, exercise ameliorated canonical phenotypes of the disease such as MBNL1 sequestration, CLC1 missplicing and myotonia²⁸. Several clinical studies in DM1 patients show that exercise results in a modest, but clinically significant improvements in strength, endurance, function and quality of life metrics, suggesting the potential of exercise as a safe treatment for DM1²⁹⁻³¹. However, what remains to be elucidated is the cellular processes that govern these benefits in humans. Unpublished data from our laboratory suggest that 12 weeks of aerobic training in adults with

DM1 is well tolerated and lead to improvements in total lean mass, muscle fibre cross sectional area, VO_{2max} and functional capacity measures). Mechanistically we observed enhanced respiration following aerobic training, increases in OXPHOS protein content, increases in mitochondrial turnover as evidenced by increases in both fusion and fission events following aerobic training. Taken together, these results suggest therapeutic potential for regular exercise in DM1 patients.

Mitochondria and DM1

DM1 patients present with multiple metabolic defects such as hyperinsulinemia, diabetes mellitus, glucose intolerance, leading to the speculation that on a molecular level there could be metabolic impairment²³. Both myoblasts and blood samples derived from DM1 patients show decreased levels of CoQ10 (a cofactor in the electron transport chain function) was negatively correlated with CUG repeat length³². Garcia-Puga and colleagues (2020) recently published work shedding light on the mechanisms underpinning a mitochondrial defect in DM1. Using patient derived fibroblasts, they show a decrease in basal respiration, max respiration, ATP production and increased levels of ROS, without any change in extracellular acidification rates (ECAR), a measure of glycolysis, in DM1. Furthermore, researchers observed a decreased phosphorylation of AKT as measured through Western blots³³. AKT is an anabolic protein that regulates insulin-dependent glucose uptake³⁴. Moreover, AKT ablation in mice show decreased ATP production, mitochondrial respiration and PGC1a expression, emphasizing the role of AKT signalling in mitochondrial function³⁵. Interestingly, when stratifying patients based on repeats >500, they found no differences between the groups³³. However, multiple measures only contained one subject in the more severe DM1 range (>500), therefore the small sample size could explain the lack of differences observed in mitochondrial measures in more severe DM1 patient fibroblasts.

DM1 fibroblasts showed no differences in the mitochondrial biogenesis markers TOMM20, PGC1- α or mitochondrial number, as compared to healthy controls, suggesting that the respiration defects are due to poor mitochondrial quality not number³³. Fibroblasts also displayed decreased expression of *OPA1*, *MFN2*, *DRP1* and *PARKIN*, suggesting dysregulation in mitochondrial dynamics and mitophagy³³. Treatment of fibroblasts with metformin, a drug known to activate AMPK and upregulate mitochondrial mass through complex I inhibition and resultant mitochondrial hormesis, ameliorated mitochondrial defects in DM1 fibroblasts³³. This data collectively shows that strategies to enhance mitochondrial function both through pharmacological and lifestyle interventions such as exercise, may ameliorate aspects of DM1 pathophysiology.

Introduction to Satellite Cells

Muscle stem cells, termed ‘satellite cells’ were first discovered in 1961 by Mauro and colleagues, and derived their name from their anatomical location between the basal lamina and sarcolemma in the muscle fibre³⁶. Muscle satellite cells (SCs) reside in a quiescent state and become activated via mechanical strain to the muscle fibre, leading to proliferation followed by either a return to quiescence, thereby replenishing the basal pool of available SCs, or differentiation into myonuclei and subsequent fusion onto the parental muscle fibre³⁷. In this manner, SCs drive myonuclear domain accretion, facilitating muscle hypertrophy by increasing the nuclei per fixed cytoplasm volume that can sustain the production of protein³⁸. Adult skeletal muscle is multinucleated by nature, where existing myonuclei are post-mitotic and therefore skeletal muscle remodelling is dependent on myonuclear increases in nuclei or replacement³⁸. In postnatal skeletal muscle, SCs are the main source of additional myonuclei making them essential for muscle maintenance, growth, and repair^{37,38}.

Myogenic Program

The specific fate of the SC, also known as the myogenic program, is tightly controlled by the expression of certain transcription factors called myogenic regulatory factors (MRFs)³⁷. During quiescence, SCs tightly regulate their myogenic program to maintain cellular quiescence and reside in G0 phase of the cell cycle³⁷. They do however express Pax7, which has become a canonical SC marker as it is specific to SCs and genetic ablation results in an absence of SCs in mouse models³⁹. Activated satellite cells exhibit an increase in transcriptional activity, as evidenced by heterochromatin uncoiling and re-entry into the cell cycle, along with an upregulation of Myf5 followed by MyoD³⁷. Activated satellite cells expressing MRFs are denoted as myoblasts. Myogenic commitment is marked by the upregulation of both MRF4 and myogenin and the concomitant downregulation of Pax7³⁷.

Satellite Cells and DM1

DM1 skeletal muscle has marked differences compared to controls. The first being a preferential atrophy of type 1 muscle fibres in distal muscles that progresses proximally⁴⁰. Muscle fibres of DM1 patients also exhibit a large range of cross-sectional area (variation in fiber size), nuclear clumping, sarcoplasmic masses, ring fibres and centrally located nuclei, all indicative of ongoing muscle regeneration⁴¹. Furthermore, intramuscular fat infiltration, fibrosis, and sarcoplasmic masses are present in DM1 muscle, suggestive of poor muscle quality⁴². It has been well elucidated in literature that SCs are indispensable for muscle regeneration and maintenance, bringing into question the role of SCs in DM1 skeletal muscle.

The CTG expansion variability present within somatic cells is referred to as somatic mosaicism, whereby various tissues express varying degrees of the mutation³. The CUG repeat is

more unstable in post-mitotic cells of skeletal muscle, cardiac tissue and the brain compared to proliferative hematopoietic cells⁴³. This suggests that the mutational burden can be present within SCs and could impact function and contribute to the observation of poor muscle quality. Additionally, that SCs may incur some protective benefit to mature muscle due to their quiescent nature that could lead to the donation of a nuclei that has accumulated less of the mutation given the appropriate stimuli.

The only study to date that has characterized SCs in DM1 human biopsies was performed by Thornell and colleagues (2009) wherein both distal and proximal muscle biopsies were taken⁴⁴. The findings from this study suggested that the number of SCs were significantly higher in distal muscles, along with greater phenotypic features of muscle pathology, whereas proximal muscles showed no differences in SC content⁴⁴. Further, they show a small proportion (~0.3-3%) of actively regenerating fibres (MyHC staining) or *de novo* fibres⁴⁴. *In vitro* experimentation with SCs explanted from skeletal muscle biopsies showed a reduction in proliferation capacity, premature growth arrest, that was independent of telomere length⁴⁴. Telomere length is important in that cells have a maximal number of divisions that can occur prior to senescing, due to the subsequent loss of upstream sequences in the lagging strand during DNA replication. In the context of SCs, shorter telomere length would imply the pathological re-entry into the cell cycle during proliferation, due to ongoing regenerative demands of the tissue, as observed in other dystrophies such as DMD⁴⁵. The absence of telomere depletion in DM1 derived SCs suggests that there is not necessarily an excessive turnover that is occurring due to regeneration, and that there are additional aberrant mechanisms that contribute to cellular senescence, which the researchers suggested as impaired autophagy. Thornell and colleagues study included a sample size of 4 DM1 patients with CTG repeats ranging from ~80 (mild DM1) to ~2420 (severe congenital cDM1), making it difficult to

draw broad conclusions regarding the spectrum of the disease⁴⁴. Furthermore, the *in vitro* methodology employed by this study for the assessment of SC proliferation was simply the total (i.e., maximal) number of cell divisions, which has been shown to not necessarily be representative of proliferative capacity, more so that of replicative cell cycle exhaustion.

While the study by Thornell and colleagues (2009)⁴⁴ stands as the first insight into the relationship between muscle SCs and the pathophysiology of DM1, there is still a marked paucity in our understanding. Indeed, subsequent *in vitro* studies have shown diverging results regarding the defects in DM1 SCs, potentially due to the large heterogeneity in the presentation of the disease. Finally, the rare nature of the disorder and the willingness for patients to undergo muscle biopsies has created studies with small sample sizes, further contributes to inconclusive results.

Failure of Proliferation in DM1 and Autophagy

There are divergent results regarding the behaviour of DM1 myoblasts in culture with one group observing an increase in proliferation⁴⁶; however, most researchers suggest a proliferation defect in SCs⁴⁷⁻⁵¹. The proliferation defect was partially rescued through the overexpression of *MBLN1* as well as deletion of nuclear foci through TALEN gene editing⁴⁸. The TALEN gene editing inserts polyA signals upstream of the triplet expansion resulting in premature transcriptional termination and has been shown to decrease defects associated with DM1 iPSCs^{48,52}.

A potential mechanism regarding the partial rescue observed with *MBLN1* overexpression is the role it plays in the inhibition of autophagy in SC through the phosphorylation of mTOR⁴⁸. Pathological increases in levels of autophagy have been previously shown in late stage DM1

myotubes as evidenced by the presence of LC3 vesicles⁵³. Elevated autophagy has suggested to be caused by the increase of p53 expression and a concomitant suppression of the mTOR pathway⁵⁴.

Autophagy is the catabolic process which uses lysosomes to degrade proteins for cellular recycling, or to be used in anabolic processes⁵⁵. Increased levels of autophagy have been shown to hinder cell proliferation by arresting the cell cycle at the G1 phase through the degradation of Cyclin D1 in cancer cells⁵⁶. However, autophagy acts as a double-edged sword as normal autophagy contributes metabolites including glucose and amino acids to cells to facilitate proliferation⁵⁵. Therefore, the fine tuning of autophagy can act as a signal for metabolic processes to occur during times of stress such as exercise or disease states. In fact, autophagy can signal the transition of myoblasts to myotubes, as myoblasts cultured in differentiation media upregulate LC3 and FOXO3, autophagic markers⁵⁷. The inhibition of autophagic flux ceases fusion and terminal differentiation⁵⁷. Furthermore, myoblasts derived from p53 knockout mouse rely heavily on glycolysis and inhibit mitochondrial biogenesis and OXPHOS leading to the inability to differentiate⁵⁷. Whether the increased autophagic markers observed in DM1 SCs can be interpreted as hindering proliferation, or simply driving differentiation has yet to be elucidated. Furthermore, in whole muscle, as discussed previously, there is evidence of AMPK activation through metformin and exercise to elicit benefits in DM1^{27,28,33}. AMPK, a catabolic protein, upregulates autophagy through the phosphorylation of ULK1⁵⁸. Based off this information, it can be speculated that levels of autophagy differ between SC and whole muscle; however, the role of autophagy and DM1 remains incompletely studied or understood.

Differentiation Defect in DM1

Along with a proliferation defect, it appears that DM1 myoblasts may also possess a differentiation impairment. Once again, mixed results persist, with Loro and colleagues (2011) observing an absence of a differentiation defect measured by fusion assays, differentiation markers at 4- and 10-days following differentiation between DM1 and control myoblasts⁵³. In contrast, cDM1 myoblasts exhibit a significantly reduced fusion index and a concomitant decrease in the differentiation markers, MyoD and myogenin⁵⁴. MyoD protein levels in myoblasts expressing mutant transcripts of 200 CUG repeats were significantly decreased; whereas, downstream myogenin signalling was intact⁵⁹. MyoD null myoblasts continued to proliferate in culture and lead to the disruption of myogenin and Mrf4 genes, indicative of its necessity for differentiation⁶⁰. The observation of downstream signalling of myogenin being normal in CUG transfected myoblasts, indicated that the defect was upstream and therefore was attributed solely to MyoD. In line with this observation, the differentiation defect was fully rescued when MyoD was overexpressed or myogenin was added, suggesting that insufficient levels of MyoD in DM1 were not able to activate myogenin⁵⁹. This is further evidenced temporally, as myogenin upregulation occurred 12 hours following MyoD activation, and results showed that 6 hours following the initiation of a differentiation protocol, MyoD levels were significantly decreased⁶¹. Additionally, DM1 myoblasts showed a decrease in the activation of p38/MAPK pathway known to phosphorylate MEF2D and lead to the recruitment of myogenin^{54,62}.

The link for how the microsatellite cell repeats leads to a SC differentiation defect could lie in the toxic gain of function of CUGBP1⁶³. CUGBP1 is differentially regulated in myoblasts compared to myotubes, potentially accounting for differentiation but not proliferation defects⁶⁴. In myoblasts, CUGBP1 is phosphorylated by AKT increasing interactions with cyclin D1 mRNA⁶⁴. During differentiation, AKT is phosphorylated by cyclin D3-cdk/6, increasing binding

with p21 mRNA and the formation of a complex with eIF2⁶⁵. In DM1, CUGBP1-eIF2 complex formation is decreased due to lower levels of cyclin D3, resulting in differentiation defects, and downregulation of myogenin and desmin⁶⁵. The reduction of cyclin D3 is due to CUG repeats increasing the activity of GSK3B, an inhibitor of cyclin D3⁶⁶. Overexpression of CUGBP1 in healthy myoblasts induced myogenic defects commonly observed in DM1 cases, and lead to less cells in the G1 phase, preventing exit from the cell cycle, indicative of a defect with terminal differentiation⁶⁷. In contrast, ablation of CUGBP1 in healthy cells lead to premature differentiation, supporting its role in cell cycle exiting⁶⁷. What remains unclear is the relationship between CUGBP1 and decreased MyoD protein levels.

RNA Toxicity and SCs in DM1

Unsurprisingly, the presence of RNA foci in SCs in DM1 has been confirmed through RNA-FISH analysis, with ~25% of SCs containing RNA foci, suggestive of RNA toxicity in SCs⁶⁸. Furthermore, MBLN1 is present in all SCs in controls; however, in DM1 SCs MBLN1 was only variably expressed⁶⁸, further underscoring the potential of foci-related impairment. Previous *in vitro* studies also confirmed the presence of MBLN1 and nuclear aggregation in myoblasts of DM1 patients⁴⁶, and in cDM1 cells⁶⁹. Using a novel mouse model of RNA toxicity, DM200, a doxycycline inducible transgenic mouse with 200 CUG repeats in the *dmpk* gene that can be induced via doxycycline supplemented in the drinking water. This mouse showed a reduction of Pax7⁺ cells per fibre, along with decreased mRNA expression of both Pax7 and MyoD, suggesting a role in RNA toxicity and the dysregulation of SCs⁶⁸. These animals displayed a delayed regenerative response in response to BaCl₂-injection induced damage, along with an inability to sustain Pax7⁺ cells following damage, implying the presence of non-functional SCs⁶⁸. Repeated

bouts of damage also showed increases in fibrosis and fat infiltration⁶⁸. Researchers suggested that the induction of RNA toxicity occurs in early differentiation as RNA foci accumulated during myotube formation but not in a myoblast stage⁴⁶. Another study using an RNA-toxicity inducing mouse model, showed that overexpression of NKX2-5, a transcription factor for cardiac progenitor development in the endoderm implicated SC function⁷⁰. NKX2-5 positively correlated with muscle histopathology, decreased SCs, inhibition of differentiation and regeneration following cardiotoxin injection⁷⁰. Furthermore, knockdown of NKX2-5 led to the rescue an expression of myogenin and p21⁷⁰. The relationship between NKX2-5 and SCs has yet to be fully elucidated. The notion that RNA toxicity leads to the over-expression of cardiac lineage markers that impair SC function, suggested the dysregulation of embryonic origins of several progenitor cells. However, it should be of note that mouse models of the disease are not always translated to humans. Taken together, these two studies indicate that RNA toxicity, could underpin the SC dysfunction observed in DM1 models.

DM1 and Premature Senescence

A consistent observation in DM1 culture studies is the premature senescence of myoblasts independent of telomere shortening^{47,50}. The lack of telomere shortening suggests that DM1 SCs are senescing not from cellular exhaustion, instead there must be intrinsic factors from the genetic mutation that lead to premature senescence. One proposed mechanism is through the overexpression of p16 due to the CUG expansion, which ultimately slows the progression of the cell cycle, as ablation of p16 was shown to rescue the growth arrest⁵⁰. Following 12 days of differentiation, myotubes showed signs of atrophy due to decreased thickness and nuclei per myofiber, increased levels of ROS production, chromatin fragmentation, cytochrome *c* and

caspace 3 cleavage, all indicative of increased apoptosis⁷¹. Another group also showed that day 10 myotubes from DM1 patients displayed greater myotube atrophy relative to controls⁴⁶.

Satellite Cells and Mitochondria

An emerging field in SC biology is the notion that mitochondrial dynamics can dictate the SC fate. Originally thought to be merely an energy deriving process involved in satellite cell dynamics, there is now evidence to suggest that the mitochondria may be actively signalling SCs through epigenetic modification by TCA intermediates⁷², ROS⁷³, mitochondrial dynamics⁷³, and mechanisms in place to actively repress OXPHOS to maintain SC identity⁷⁴.

The myogenic program can be mapped metabolically with SCs relying on mitochondrial fatty acid oxidation during quiescence and to a lesser extent OXPHOS⁷². The reliance on fatty acid oxidation results in high levels of NAD⁺ that induces SIRT1 mediated deacetylation of K4k16, ultimately inhibiting transcription of the myogenic program to maintain quiescence⁷⁵. Furthermore, a study by Rochateau and colleagues (2012), denoted two distinct subpopulations of quiescent SCs. One population that displayed high Pax7 expression, low mitochondrial density, and ATP, were predisposed to exhibit a proliferative phenotype⁷⁶. The second population showed low Pax7, high mitochondrial density and ATP, displayed higher levels of differentiation markers such as myogenin, Sca1 and desmin⁷⁶. This provided additional evidence that mitochondrial density plays a role in dictating SC fate. Proliferation and activation are marked by the metabolic shift towards glycolysis⁷⁷. The shift towards anaerobic metabolism enables *de novo* synthesis of nucleotides, lipids and proteins which ultimately support the SCs needs for growth⁷². A similar shift is observed in cancer cells, which rapidly proliferate, called the Warberg shift⁷⁸. Interestingly, in SCs, AMPK knockout cells, causes the reliance on glycolysis and thereby increasing

proliferation⁷⁹. Mice genetically modified to have a specific AMPK knockout in the myofiber but not the SC, did not modulate the myogenic program⁷⁹. This suggests that AMPK deficiency in the niche does not regulate SC fate, instead, intrinsic metabolic disturbances of the SC drive fate determination. During differentiation, SCs rely heavily on OXPHOS and to a lesser degree fatty acid oxidation^{72,73}. Knockout of SIRT1 in SCs, a gene implicated in mitochondrial biogenesis, resulted in premature differentiation as evidenced by an increase in differentiation markers and impaired muscle regeneration⁸⁰. Furthermore, Pala and colleagues (2018) uncovered that extracellular acidification rate (ECAR, a measure of glycolysis) was highest in SCs isolated from skeletal muscle 3 days post-injury, where peak activation occurred suggesting glycolysis prevailed during activation⁸¹. Following 5 days post-injury oxygen consumption rate (OCR, a measure of mitochondrial respiration) remained elevated whereas glycolysis tapered off⁸¹. This suggested that the transition towards OXPHOS, and the downregulation of glycolysis only may be required to maintain quiescence.

Shintaku and colleagues (2016) uncovered the first direct link between MRFs and mitochondria as they discovered through genome wide analysis of transcription factors of skeletal muscle cells that MyoD, which binds to myogenin to induce differentiation, also binds to multiple genes involved with mitochondrial biogenesis, fatty acid metabolism, mitochondrial fission and OXPHOS⁸². Furthermore, MyoD ablation in myotubes and knock out mice resulted in lower mitochondrial respiration. Moreover, genetic knockout of MyoD also significantly reduced TCA cycle activity and β -oxidation as shown using radiolabeled substrates⁸². MyoD null mice also show a decrease in PGC1 α isoforms, a master regulator in mitochondrial biogenesis⁸². This study emphasized the importance of MyoD in mitochondrial maintenance and function.

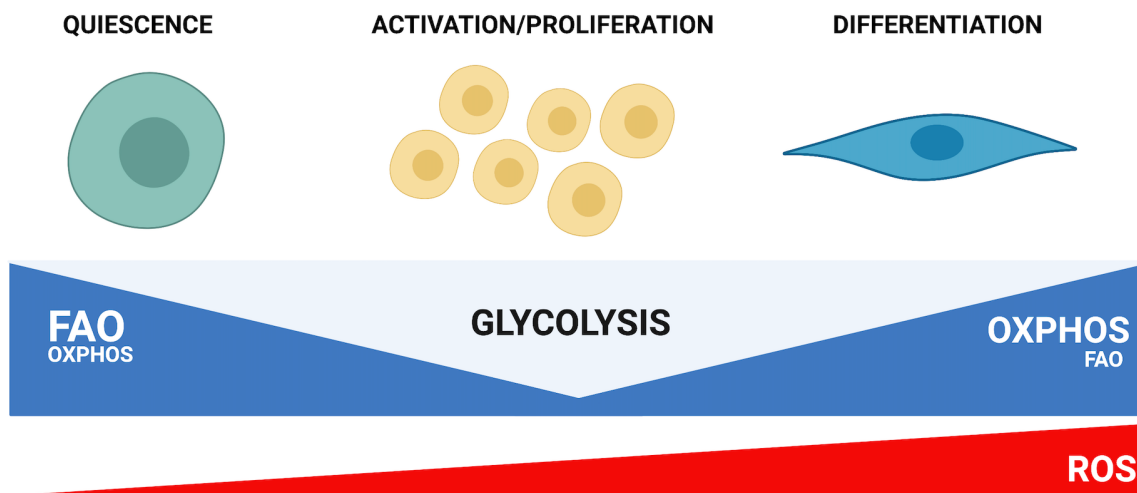


Figure 1. Metabolic Orchestration of Myogenic Program

Satellite Cell and Mitochondria- Implications for Muscular Dystrophies

This relationship between mitochondria and satellite cells is further supported by the observation that other metabolic diseases with altered mitochondrial function also show changes in SC function. Mitochondrial dysfunction is well characterized in Duchenne muscular dystrophy (DMD) and has been shown to precede muscle atrophy due to reduced dystrophin⁸³. Mouse models for muscular dystrophy (*mdx*) show an increased number of satellite cells due to an ongoing cycle of regeneration followed by degeneration, ultimately leading to cellular exhaustion⁸⁴. Myoblasts from *mdx* mice displayed decreased oxygen consumption rates, expression of ETC complexes and membrane potential as well as increased glycolytic rates and ROS⁸⁵. Restoration of dystrophin through CRISPR/Cas9 showed concomitant normalizing of OXPHOS, and proliferation and differentiation activity of *mdx* myoblasts⁸⁶. As discussed previously, DM1 fibroblasts show mitochondrial dysfunction, as evidenced by lower oxygen consumption rate, increased levels of ROS, lower ATP production³³. Moreover, mouse models of DM1 show lower OXPHOS protein²⁸, and a decrease in AMPK activation²⁷- further indicating mitochondrial dysfunction. Human work

shows low levels of CoQ10 in the blood, a cofactor in the electron transport chain,³² and unpublished work from our own laboratory suggests lower OXPHOS protein content as well as impaired mitochondrial respiration. Taken together, we speculate that mitochondrial disturbances present in DM1 may contribute to the dysregulation of the myogenic program observed in literature. To our knowledge, no studies have investigated mitochondrial respiration in DM1 primary myoblasts.

Thesis Purpose, Objectives, Hypothesis

Satellite cells in DM1 patients have yet to be fully investigated, signifying a critical gap in the literature as SCs are imperative to muscle health and likely contribute to the myopathy of the disease. The presence of both muscle atrophy and centrally located nuclei suggest a dysfunction in SCs in DM1 patients. Currently, only one study exists in DM1 patients, where the sample size was small (n=4) and therefore results may not be representative of the broader DM1 population. Furthermore, SCs are known to respond readily to exercise training, and retain their capacity to respond to exercise in both aging and disease states. This suggests therapeutic potential of exercise on SC behaviour, which has yet to be investigated in literature. Furthering our understanding on the cellular mechanisms contributing to DM1 myopathy is important because it may assist in the development of additional therapeutic avenues in which lifestyle and pharmacological interventions may mitigate the disease.

Therefore, the primary aim of the present study was to characterize SC content in 11 DM1 patients at baseline and following 12 weeks of aerobic training. Secondary aims include investigating components of the niche, and mitochondria as potential mechanisms underlying SC dysfunction.

The specific objectives were to:

- 1) Characterize both the Pax7⁺ (basal pool of SCs) and Pax7⁺/MyoD⁺ (activated pool of SCs) cells in DM1 skeletal muscle at baseline and following training
- 2) Investigate niche components such as capillaries, presence of fibrosis and fat infiltration, all of which have been implicated to perturb SC function. Moreover, whether exercise training ameliorates these measures.
- 3) Examine whether SCs possess the CUG foci and whether the mutational load changes with exercise training.
- 4) Examine metabolic defects in glycolysis and mitochondrial respiration *in vitro* that could contribute to myogenic defects

We hypothesized that SCs in DM1 would be dysfunctional due to indices of poor muscle quality observed in muscle cross sections. We hypothesize that SC pool will increase following training to support hypertrophy because in unpublished data from the same study, we observed a significant increase in type 2 muscle cross sectional area. Furthermore, we hypothesized that exercise training would induce beneficial effects on components of the niche such as vascularization, fibrosis, and fat infiltration.

MANUSCRIPT

TITLE: Characterization of satellite cells and associated myogenic defects in DM1 with aerobic training.

AUTHORS: Katherine Manta¹, Andrew Mikhail², Jack Puymirat³, Mark A. Tarnopolsky¹, Joshua P. Nederveen¹

INSTITUTIONS:

¹Department of Pediatrics, McMaster University Medical Center (MUMC), Hamilton, Ontario, Canada

² Department of Kinesiology, McMaster University, Hamilton ON, Canada

³ Department of Medicine, CHU Research Centre of Quebec, Laval University, Laval, ON, Canada

Introduction

Myotonic dystrophy type 1 (DM1) is the most common adult-onset muscular dystrophy affecting 1:8000 individuals worldwide with prevalence rates as high as 1:600 in part of Northeastern Quebec^{1,4}. A recent study suggests that the genetic prevalence of the disorder as detected by CTG repeat expansion screening is fourfold higher than the previous estimate, emphasizing the widescale prevalence of the disorder⁵. Patients with DM1 have multisystemic defects; however, skeletal muscle hallmarks include weakness and atrophy that progresses in a distal to proximal fashion, and myotonia, (sustained hyperexcitability of skeletal muscle)^{2,23}. The disorder is caused by the autosomal dominant inheritance of a CTG triplet repeat expansion in the 3' untranslated region of the DMPK gene, whereby the number of repeats correlates positively with both the severity and onset of the disorder^{1,2,23}.

The microsatellite expansion causes the formation of hairpin structures that are stabilized by both Watson-Crick base pairing and intramolecular forces¹. This hairpin structure ultimately leads to the alteration of two major proteins: MBLN1 and CUGBP1¹. These repeats are not able to exit the nucleus and reach the cytoplasm leading to hallmark phenotypic “foci”, or retention of mutant mRNA widely observed in DM1^{15,16}. Furthermore, the triplet repeat mutation causes dysfunction at all levels of cell including chromatin structure and function, replication, transcription, mRNA processing, translation and signalling, leading to the multifaceted defects associated with the disorder¹⁴.

DM1 skeletal muscle has notable characteristics as compared to healthy controls. The first being a preferential atrophy of type 1 muscle fibres in distal muscles that progresses proximally⁴⁰. Muscle fibres of DM1 patients also exhibit a large variation in fiber size, nuclear clumping, sarcoplasmic masses, ring fibres and centrally located nuclei, indicative of ongoing muscle

regeneration⁴¹. DM1 muscle also shows markers of overall poor muscle quality such as fat infiltration, fibrosis and sarcoplasmic masses⁴².

At the heart of muscle maintenance, regeneration and repair is the muscle stem cell, coined the satellite cell (SC)⁸⁷. SCs reside between the basal lamina and sarcolemma of muscle fibres in a quiescent state³⁷. Following activation, due to mechanical strain of skeletal muscle such as from injury or exercise, SCs proliferate to replenish the pool of available SCs or differentiate into myonuclei followed by subsequent fusion onto the parental muscle fibre⁸⁷. In postnatal skeletal muscle, SCs are the only source of an additional myonuclei, making them indispensable for muscle regeneration and hypertrophy³⁸. Considering their pivotal role in skeletal muscle remodeling and maintenance, it brings into question the role that SCs contribute to DM1 myopathy.

Surprisingly, to date, there is only one study that has characterized SCs in DM1 skeletal muscle biopsies showing an elevated pool in distal but not proximal skeletal muscle⁴⁴. Furthermore, multiple *in vitro* studies suggest both a proliferation^{44,48,51,88} and differentiation defect^{59,59,65,89,90} in patient derived myoblasts, although divergent results have been observed. Taken together, along with the observation of poor muscle quality, these results show that the myogenic program in SCs is dysregulated in DM1.

Therefore, the aim of the present study was to extensively characterize SCs in 11 DM1 patients before and following aerobic training. Exercise training is a potent stimulator of the myogenic program, and studies suggest that it is both well tolerated in DM1 patients and elicited a therapeutic benefit in DM1²⁷⁻³¹. Furthermore, we sought to characterize components of skeletal muscle quality, widely shown in literature to modulate SC behaviour. Finally, we suggest mitochondrial impairments in DM1 may underpin SC dysfunction and provides a therapeutic avenue for aerobic training in patients.

Methods

Ethical approval

This trial was approved by the Hamilton Integrated Research Ethics Board (#7091) and the study complied with the guidelines set out in the Canadian Tri-Council policy statement on ethical conduct for research involving humans. Written informed consent, regarding the risks and nature of the experimental procedures, was obtained from all participants prior to any study interventions. This study was registered on clinicaltrials.gov under study #: NCT04187482.

Participants

Patients were recruited from the Neuromuscular and Neurometabolic Clinic at McMaster University Medical Center (MUMC). All DM1 patients were considered for this trial, upon meeting eligibility criteria, a total of 13 DM1 patients were interested in participating. Two participants dropped out after week 2 of the trial for personal reasons unrelated to the study. A total of 11 patients with DM1 (5M and 6F; age 42.5 ± 2 years; mean \pm SEM, $n = 11$) completed the trial and were included in the study results. Details regarding participant characteristics are outlined in Table 1. Eleven age and sex matched (5M and 6F) healthy controls were recruited from the Hamilton community for baseline comparisons. All participants were sedentary (performing < 2 h of structured aerobic activity per week) and were asked to refrain from any additional exercise during the duration of the intervention outside of that prescribed (see below). Exclusion criteria including smoking, diabetes (type 1 or 2), cardiovascular or respiratory disorders (other than a mild restrictive ventilatory defect and/or a borderline first degree heart block (< 210 ms)), other known genetic disorders, active musculoskeletal injuries or any other health complications that would hinder their ability to perform regular aerobic training.

Table 1. Participant Characteristics and Adherence

<i>Subject</i>	<i>Sex</i>	<i>Age</i>	<i>CTG Repeats</i>	<i>Weight (kg)</i>	<i>Height (m)</i>	<i>Adherence</i>
1	M	26	650	80.3	1.88	34/36
2	F	50	800	71.5	1.67	36/36
3	M	50	650	53.3	1.76	36/36
4	M	43	400	77.9	1.76	36/36
5	F	27	500	78.9	1.66	18/36
6	F	49	900	50.9	1.53	36/36
7	M	47	900	52.6	1.63	36/36
8	F	39	300	91.6	1.71	34/36
9	F	40	900	47.3	1.60	36/36
12	M	53	800	85.3	1.82	36/36
13	F	45	300	59.5	1.52	35/36
<i>AVG</i>		42.6 ± 2	645 ± 71	68.1 ± 4.8	1.68 ± 0.03	

Training Intervention

Participants trained 3 times per week for a total of 12 weeks on a stationary bicycle (Lode, Groningen, Netherlands). The training sessions began with a 3-minute warmup at a resistance of 25 watts, followed by 30 minutes of exercise training performed at 65% of max workload determined via VO_{2peak} test (W_{peak}) performed prior to the intervention, followed by a 2 minute cool down at 25 watts. Training intensity progressively increased to 35-min at 75% W_{peak} by week 12. All training sessions were completed in the Neuromuscular and Neurometabolic Clinic and supervised by a trained professional with hospital staff on site.

Muscle Biopsies

Participants underwent a muscle biopsy of the distal 1/3 of the vastus lateralis following an overnight fast (~10 hours) as described previously⁹¹. Subjects were told to arrive fasted as well as refrain from any physical activity 96-hours prior to the biopsy. Biopsies were obtained pre- and

post- intervention for patients with DM1 and only baseline for controls. Approximately 150 mg of muscle tissue was collected from each biopsy. Pre- and post- intervention biopsies were taken from opposite legs at approximately the same distance from the joint to limit the potential effect of the antecedent biopsy. Following collection of the sample, the muscle was dissected free of adipose and connective tissue (if necessary) and flash-frozen in liquid nitrogen, then stored at -80°C for later analysis.

Immunohistochemical Staining

Cross sections of $7\mu\text{m}$ were prepared from muscle biopsies embedded in OCT using a cryostat at -20°C , air-dried and then stored at -80°C . Prior to staining, slides were allowed to come to room temperature and condensation was removed using a KimTech wipe. Samples were traced with a PAP pen and allowed to dry for an additional 15 minutes to prevent the loss of liquid. For SC and capillary staining the following procedure was used. Slides were fixed with 4% PFA (PFA, Sigma-Aldrich) for 15 minutes at room temperature, followed by a 3x5 minute wash in 1xPBS. Sections were then incubated in blocking solution for 1 hour and a half at room temperature consisting of 2% bovine serum albumin, 5-10% goat serum, 0.2% Triton X-100. Following blocking, slides were incubated with primary antibodies in a humidified chamber at 4°C overnight. Detailed primary and secondary antibody concentrations are listed in Table 2. Following secondary antibody incubation, slides were immediately cover-slipped using DAKO and DAPI solution and dried in the dark overnight. To evaluate SC content in DM1 muscle, immunohistochemical staining was employed on muscle cross sections from patient using a SC canonical marker, Pax7, overlaid with DAPI to denote SCs⁹². Percent of activated satellite cells were quantified by MyoD⁺/Pax7⁺ cells per total Pax7⁺.

For perilipin/BODIPY™ staining an adapted protocol was used. Slides were fixed in 4% formaldehyde for 20 minutes, washed and blocked with 2% BSA, supplemented with 0.02% triton for 1 hour, and permeabilized 0.3% Triton X in PBS for 5 minutes. Perilipin was diluted in 2% BSA and 0.02% percent triton and incubated on slides for 1 hour at 37°C in a humidified incubator. BODIPY™ was added with the secondary antibodies at a concentration of 1:1000 for 1.5 hours at 37°C. Slides were dried and cover slipped using DAKO.

For eMHC staining dried slides were not fixed and immediately incubated in blocking solution consisting of 10% goat serum in PBS with 0.2% Tween 20 (Sigma-Aldrich) for 30 minutes at room temperature. Primary antibody was added 1:10 in 2% bovine serum albumin and incubated at 37 degrees in a humidified incubator for 30 minutes. Slides were then treated with secondary antibody, dried and cover-slipped.

Slides were imaged on the 20x objective using Nikon Eclipse *Ti* Microscope (Nikon Instruments, Inc., Melville, NY, USA), equipped with a high-resolution Photometrics CoolSNAP HQ2 fluorescent camera (Nikon Instruments). Images were blinded and quantified using Nikon NIS Elements AR 3.2 software (Nikon Instruments) by the same researcher.

To give an overview of capillarization in muscle fibres, the number of capillary contacts (number of capillaries around a muscle fibre), capillary density per area and per muscle fibre, and the capillary fibre perimeter exchange index (CFPE) was calculated as an estimate to muscle perfusion in muscle cross sections⁹³. Capillaries were evaluating using immunohistochemistry using CD31 as a marker for capillaries.

Table 2: Antibody information for staining muscle cross sections

<i>Primary</i>	<i>Species</i>	<i>Source</i>	<i>Concentration</i>	<i>Secondary</i>	<i>Concentration</i>
<i>PAX7</i>	Mouse	DSHB	1:2	Alexa 594 goat-anti mouse	1:500

<i>MyoD1</i>	Rabbit	Cell Signalling Technologies 13812	1:400	Alexa 488 goat-anti rabbit	1:500
<i>CD31</i>	Rabbit	Abcam ab11575	1:40	Alexa 647 goat-anti rabbit	1:500
<i>Laminin</i>	Rat	Sigma- Aldrich L0663	1:200	Alexa 647 goat-anti rat	1:500
<i>MHC1</i>	Mouse	DSHB A4.951 slow isoform	Neat	Alexa 647 goat-anti mouse	1:500
<i>Perilipin</i>	Rabbit	Cell Signalling Technologies, 9349S	1:250	Alexa 594 goat-anti rabbit, WGA 647	1:500
<i>BODIPYTM</i>	n/a	Thermo Fisher Scientific, D3922	1:1000	n/a	n/a
<i>eMHC</i>	Mouse	DHSB, Bf-F6	1:10	Alexa 488 goat anti-mouse, WGA 647	1:500

Histochemical Staining

Masson's Trichrome staining was performed using 7 µm muscle cross sections, air dried for 3 hours in a fume-hood. Slides were fixed with 4% PFA for 1 hour, followed by subsequent fixation with Bouin's fixative (Sigma-Aldrich, St. Louis, MO, USA) overnight at room temperature. Slides were washed with water, incubated with Weigert's iron hematoxylin for 5 minutes, washed again, and incubated in Biebrich scarlet-acid fuchsin for 5 minutes. Slides were placed in phosphomolybdic-phosphotungstic acid (3 × 3 min), incubated in aniline blue for 5 minutes, washed, and incubated in 1% of glacial acetic acid for 2 minutes. Slides were treated with graded ethanol washes, then, cover-slipped. Images were taken at × 20 by using Nikon DS-Fi1. To determine the extent of fibrosis, threshold analysis was employed to determine the area occupied by blue staining as a measure of the total area of the muscle section using Nikon NIS-Elements 3.2 AR software.

Protein Extraction and Immunoblotting in vivo

Muscle chips of 20 mg were pulverized using a Cell Crusher (Cork, Ireland) and subsequently homogenized using 200 μ L of RIPA lysis buffer (ThermoFisher Scientific, 89901) supplemented with protease and phosphatase inhibitor cocktail (Halt™, ThermoFisher Scientific, 78440). Samples were mechanically homogenized using a FastPrep 24 5G (MP Biomedicals, Santa Ana, California, USA) for 3 cycles consisting of 45 seconds at 6 m/s with a one-minute on-ice incubation in between repetitions. Following homogenization, protein lysates were incubated on ice for 1 hour on a shaker plate. Samples were then centrifuged at 14,000 g for 15 minutes at 4°C, where the supernatant was collected, and the pellet was discarded. Protein concentrations were determined using a BCA Protein Assay Kit (Pierce, Thermo Scientific, 23225), diluted 10X. The microplate procedure was used with 10 μ L of sample loaded per a well and using a plate reader at an absorbency of 562 nm. Protein lysates were prepped in 6X Laemmli Buffer (Fisher Scientific, AAJ61337AC), normalized for concentration and volume across samples, and heated for five minutes at 95°C using a heat block (VWR Scientific, ON, Canada). 10 μ g of protein was loaded on a 4-20% Criterion TGX Precast Midi Protein Gel (Bio-Rad Laboratories, 5671094) with a PageRuler Plus Prestained Protein Ladder Protein Ladder, 10 to 250 kDa (Thermo Fisher, 26619), and protein content was determined via standard SDS-page run at 70V for 10 minutes, followed by 120 V for 1 hour and half. Gels were then transferred on a nitrocellulose membrane at 25 V for 15 minutes. Commercially available Ponceau S solution (Sigma Aldrich) was used to confirm equal protein loading. Membranes were subsequently blocked using 5% bovine serum albumin (BSA) for one hour at room temperature. Primary antibodies were prepared with 5% BSA at the following concentrations (MyoD1, CST 13812, 1:1000; PAX7, DHSB, 0.3 μ g/mL; Myogenin, DHSB myogenic factor 4, 0.3 μ g/mL) overnight in a cold room. Secondary antibodies Donkey

Anti-Rabbit IgG Antibody Peroxidase and Donkey Anti-Mouse IgG Antibody Peroxidase (Jackson ImmunoResearch) for one hour at room temperature. Blots were imaged using Clarity Western ECL substrate (Bio-Rad Laboratories, 170-5061) containing 50% Luminol/enhancer and 50% peroxide solution for 10 minutes. Membranes were developed using ChemiDoc MP Imaging System (Bio-Rad Laboratories, CA, USA). Intensities of the bands were quantified using Image Lab Software 5.1 (Bio-Rad Laboratories, CA, USA) and normalized to whole lane Ponceau S staining and across blots using a multi-gel control. Statistical analysis was carried out on normalized values for each protein of interest.

Fluorescent in Situ Hybridization (FISH)

Muscle cross sections (7 μm in thickness) were stored at -80 and allowed to come to room temperature prior to beginning the stain. Sections were fixed with 4% PFA for 30 minutes followed by a five 2-minute washes in PBS. Slides were then incubated in ice-cold 2% acetone in PBS 5 minutes. Following acetone incubation, slides were incubated with prehybridization buffer (2x SSC, 30% formamide in water) for 10 minutes at room temperature. For hybridization, slides were incubated in the probe consisting of 30% formamide, 2x SSC, 1% BSA, 1 mg/mL yeast tRNA, vanadate, and the CUG probe (a generous gift from Dr. Vladimir Ljubcic) diluted to 1 ng/ μl in water for 2 hours at 37°C in a wet chamber. Following hybridization, slides were placed in a hot wash at 45°C in prehybridization buffer for 30 minutes. Slides were then washed in a 1xSSC solution in MilliQ water at room temperature for 30 minutes. Immunohistochemical staining was then carried out using PAX7, laminin and DAPI using the protocol described above. Images were taken using Olympus Fluoview 2100 confocal microscope using a 60x oil emersion lens. SCs were manually located, and a z-stack was taken of the entire muscle section thickness to observe any

CUG repeat overlay. Images were quantified using ImageJ software, where the number of nuclei was thresholded, the SC counts and CUG positive nuclei as well as SCs was done by manually counting.

Cell Culture

Cell cultures were obtained in collaboration with CHU Research Centre of Quebec BioBank from Dr. Jack Puymirat. Control cell lines (HSMM) were purchased from Lonza (CC-2580). Table 3 described patient characteristics of myoblasts. Myoblasts were cultured and maintained in a humidified incubator at 37°C and 5% CO₂ in culture medium. Cell media consisted of Hams F10 nutrient mix (Thermo Fisher Scientific) supplemented 20% fetal bovine serum (Thermo Fisher Scientific), 0.4 ug/ml dexamethasone (Sigma-Aldrich), 10 ug/ml of FGF, 5ug/ml of insulin and 1% penicillin streptomycin (Thermo Fisher Scientific). Media was changed every other day and cells were passed once they reached approximately 70% confluency.

Table 3. *In vitro* myoblast characteristics

<i>Cell lines</i>	<i>Type</i>	<i>Age at biopsy (years)</i>	<i>Sex</i>	<i>CTG</i>
<i>CTRL-1</i>	CTRL	0	F	n/a
<i>CTRL-2</i>	CTRL	21	M	n/a
<i>DM1-1</i>	DM1	34	M	300
<i>DM1-2</i>	DM1	27	M	1300
<i>DM1-3</i>	DM1	38	M	350

Proliferation Protocol

Myoblasts were seeded at 5000 cells per well of a sterile 96 well plate for MTT assay. After 72 hours the Vybrant MTT Cell Proliferation Assay Kit (Thermo Fisher Scientific, V13154) was performed as per manufacturers instruction for MTT labelling with DMSO. Raw values of DM1

cells were obtained via a plate reader set at 540 nm and were normalized to the average of the control.

For BrdU staining, which labels cells actively undergoing S-phase, cells were plated in triplicates in a 12 well dish at 5000 cells/cm² in 1 mL of culture medium. After 72 hours, BrdU was added to the cells (Thermo Fisher, B23151) at a final concentration of 10 µM for 2 hours at 37°C. Subsequent staining was performed as per manufacturer's instructions and labeled with conjugated Brdu monoclonal antibody (1:1000, Thermo Fisher Scientific, B35130), DAPI and cover-slipped. Three non-overlapping images were taken using Olympus Fluoview 2100 confocal microscope on the 10x objective with a 4.0x zoom. Double-positive DAPI/BrdU cells were quantified using ImageJ software as a fraction of total cells. Data was then normalized to the average of the controls.

Differentiation Protocol

To induce differentiation in myoblasts, at confluency, media was switched on all plates to differentiation media (Hams F10 media supplemented 6% horse serum, 0.4 µg/ml dexamethasone (Sigma-Aldrich), 10 µg/ml of FGF, 5µg/ml of insulin and 1% penicillin streptomycin (Thermo Fisher Scientific) and changed every other day. Cells were collected 4-, 6-, 8- days following media switch for subsequent staining, mRNA and protein analysis.

Immunofluorescence

Cells were plated in triplicate on 12-well plates coated with Matrigel at 5000 cells/cm² and allowed to grow to confluency prior to switch of differentiation media. Cells were fixed with 4% PFA for 15 minutes, washed 3 times and stored at 4°C in PBS to enable synchronization of all

differentiation time points. Prior to staining, cells were allowed to equilibrate to room temperature and cells were incubated in permeabilization buffer consisting of 0.1% Triton-X in PBS for 20 minutes at room temperature. Cells were subsequently blocked in 2% BSA for an hour, followed by incubation of primary antibodies overnight at 4°C. Desmin (1:1000, Invitrogen, PA5-115113) and myogenin (1:50, DHSB myogenic factor 4) were diluted in 2% BSA. Secondaries were added 1:1000 (Alexa 594 goat anti-rabbit, Alexa 488 goat anti-mouse) in 2% BSA for 2 hours at room temperature. Cells were washed and cover-slipped with DAPI and DAKO for imaging. Three non-overlapping images were taken using the Olympus Fluoview 2100 confocal microscope on the 10x objective with a 2.5x zoom. Fusion index was quantified using MyoCount software and number of Myogenin/DAPI cells were quantified using ImageJ software.

Immunoblotting and Protein Extraction in vitro

Myoblasts were plated in a 6-well plate at a density of 10000 cells/cm² and allowed to grow for three days prior to protein extraction. Cells were washed 1x with sterile PBS, followed by the addition of 200 uL of RIPA lysis buffer (ThermoFisher Scientific, 89901), supplemented with protease and phosphatase inhibitor cocktail (Halt™, ThermoFisher Scientific, 78440) per well. Plates were stored at -80°C for protein extraction at a later time, thawed and scraped and treated to a similar to protein and immunoblotting protocol listed above. Table 3 outlines detailed antibody concentrations used for western blotting.

Table 4. Antibody Information for western blotting *in vitro*

<i>Primary</i>	<i>Species</i>	<i>Source</i>	<i>Concentration</i>
<i>OXPPOS</i>	Mouse	Abcam, ms604	1:2000
<i>SOD1</i>	Rabbit	Abcam, ab51254	1:1000
<i>SOD2</i>	Rabbit	Abcam ab11575	1:1000
<i>P-GSK</i>	Rabbit	Cell Signalling Technologies, 9323T	1:10,000
<i>T-GSK</i>	Rabbit	Cell Signalling Technologies, 9315S	1:5000

<i>P-AMPK</i>	Rabbit	Cell Signalling Technologies, 2531	1:2000
<i>T-AMPK</i>	Rabbit	Cell Signalling Technologies, 2532	1:2000
<i>CS</i>	Rabbit	Abcam, ab96600	1:2000
<i>OPA-1</i>	Rabbit	Abcam, ab42364	1:5000
<i>DRP-1</i>	Rabbit	Cell Signalling Technologies, 8570S	1:1000
<i>PGC1a</i>	Mouse	Calbiochem, KP9803	1:1000
<i>MFN1</i>	Rabbit	Cell Signalling Technologies, 14739	1:1000
<i>MFN2</i>	Mouse	Abcam, ab56889	1:5000
<i>P62</i>	Rabbit	Cell Signalling Technologies, 5114S	1:1000
<i>MBLN1</i>	Rabbit	Santa Cruz Biotechnology, sc47740	1:1000
<i>GAPDH</i>	Rabbit	Invitrogen, PAI-987	1:1000
<i>P-ACC</i>	Rabbit	Cell Signalling Technologies, 14739	1:2000
<i>T-ACC</i>	Rabbit	Cell Signalling Technologies, 14739	1:2000
<i>FIS1</i>	Rabbit	ProteinTech, 10956-1-AP	1:1000

Metabolic Measurements

Oxygen consumption rate (OCR) and extracellular acidification rate (ECAR) was performed in XFe24 plates using the Seahorse XFe24 Analyzer (Agilent). Myoblasts were seeded at 40,000-50,000 cells per well in triplicates with 250 ul of culture medium, for 24 hours prior to performing the assay. For myotube experiments, myoblasts were seeding at 40,000-50,000 cells in 250 ul of culture medium in a Matrigel coated XFe24 plate. The following day, media was switched to differentiation media and replaced every other day until the experiment. Myotubes measurements were performed on 6-day old myotubes. OCR was evaluated using the *Seahorse XF Cell Mito stress Test Kit*, according to manufacturer's instructions (Agilent). ECAR was measured in an adapted protocol using 2 mM D-glucose (Sigma-Aldrich), 5 uM Oligomycin (Sigma-Aldrich) and 2mM of 2-Deoxy-D-glucose (Sigma-Aldrich), following a titration curve. All values were normalized to protein concentration as determined by homogenization in 100 ul per well of RIPA lysis buffer (ThermoFisher Scientific, 89901) and subsequent BCA Protein Assay Kit analysis (Pierce, Thermo Scientific, 23225).

Statistical Analysis

All *in vitro* statistics were carried out using a one-way non-parametric ANOVA analysis, comparing the means of DM1 Pre and Post to that of the CTRL and a Fisher LSD post-hoc test was employed to enable multiple comparisons. Furthermore, paired Student's *t*-test was employed for DM1-Pre and DM1-Post to elucidate any exercise effects within the group.

For cell culture, a nonparametric Student *t*-test was employed to investigate statistical differences between DM1 cell cultures and CTRL. Experiments were carried out in triplicates where each triplicate was included in the analysis.

Results

First, we characterized both basal (Pax7⁺) and activated (Pax7⁺/MyoD⁺) SC pools in DM1 muscle cross sections. Our results show a significant 2.24- and 1.84- elevation of type 1 and type 2 associated SCs, respectively, in DM1 muscle ($p < 0.05$, Fig. 1B). The type 2 associated SC display a further 1.40-fold increase following aerobic training ($p < 0.05$, Fig. 1B). There is no difference in the percentage of MyoD⁺/Pax7⁺ cells at baseline in DM1 vs controls, with no training effect observed (Figure 1C). In accordance with immunohistochemical results, we show a concomitant 1.54- and 1.83- fold higher Pax7 protein content in DM1 Pre and Post samples ($p < 0.05$, Figure 1E), respectively, with no significant differences in MyoD protein content between groups (Figure 1D). Additionally, DM1 shows a 1.44- and 1.48- fold higher myogenin protein content compared to the controls, with no effects of training ($p < 0.05$, Figure 1E).

Nuclei per myofiber area, an indicator of myonuclear domain, was measured in 25 type 1 and 25 type 2 skeletal muscle fibres⁹². Results indicate that DM1 muscle exhibit a trend for a greater number of nuclei per type 1 muscle fibre vs. controls ($p = 0.07$), with no significant differences in type 2 fibres or with training (Figure 1G).

DM1 muscle exhibits numerous centrally located nuclei as compared to control subjects, indicative of ongoing muscle regeneration. To further evaluate muscle regeneration, the presence of embryonic myosin heavy chain (eMHC) fibres was stained for in all subjects. Approximately 1.62% and 2.5% of DM1 skeletal muscle at baseline and following training possess eMHC; whereas, there was an absence of these fibres in all control subjects. The higher amount of eMHC did not reach significant ($p=0.06$, Figure 1H), potentially due to their relatively rare nature in muscle sections.

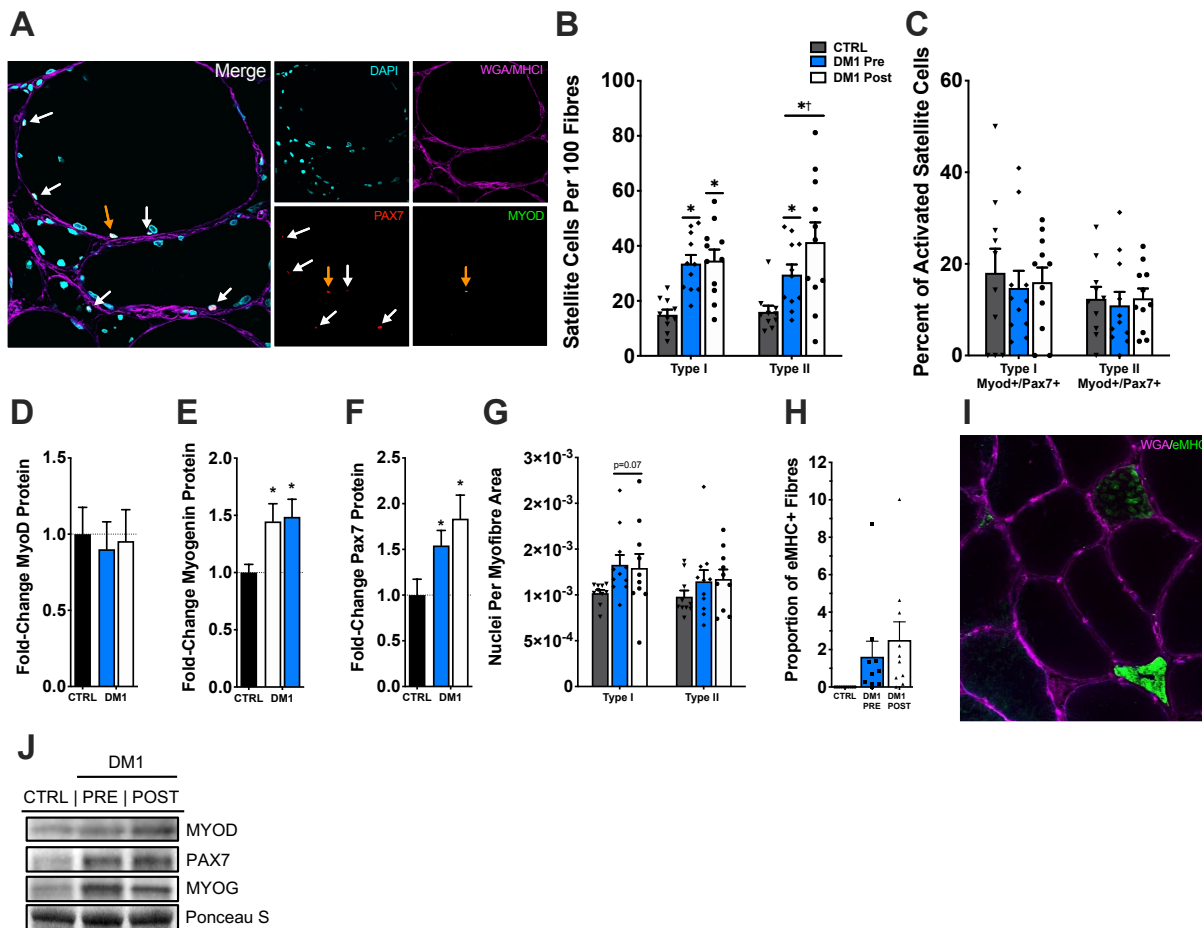


Figure 1. DM1 muscle exhibits increased satellite cell pool, and fusion markers.

(A) Representative image of PAX7/DAPI/MYOD/WGA/MHC1 stain in DM1 skeletal muscle. White arrows point to PAX7⁺ cells, whereas the orange arrow points to a

MYOD⁺/PAX7⁺ cell (A). (B) Characterization of fibre-type specific PAX7⁺ cells per 100 fibres in CTRL and DM1 with training. (C) Quantification of the percent of MYOD⁺/PAX7⁺ with respect to total PAX7⁺ cells in a fibre-type specific manner. Fold-change of protein content in DM1 muscle homogenates relative to CTRL of MyoD (D), myogenin (E) and PAX7 (F), as measured through Western blot analysis. (G) Fibre type specific myonuclear domain as quantified by the number of nuclei per individual myofiber area. (H) Quantification of the number of positive fibres for eMHC relative to the total fibres per muscle cross section. (I) Representative image of positive eMHC fibres in DM1 muscle (green), absent in CTRL. (J) Representative Western blots of myogenic markers (D-F). Values represent means \pm SEM; * $P < 0.05$ significant DM1 vs CTRL, obtained through one-way ANOVA with a Fisher LSD post-hoc test; † $P < 0.05$ significant DM1PRE vs POST using a paired t-test ($n=11$).

The elevation of the satellite cell pool and the presence of markers of regeneration, in the face of overall poor muscle quality and atrophy, suggests that the satellite cells are dysregulated. This observation led us to examine whether the genetic CUG triplet repeat expansion, that displays heterozygous presentation in various cells, is present in satellite cells and to what degree. We employed FISH/IF techniques to determine the colocalization of (CUG)_n probe in Pax7⁺ cells. The use of (CUG)_n probe with FISH to detect nuclear foci is well documented in multiple studies and an adapted protocol was used^{20,28,94-96}. The (CUG)_n probe was not present in any of the control SCs, providing validation for the method employed. In DM1, approximately 31% of SCs at baseline and 37% of SCs following training were positive for the CUG triplet nuclear expansion (Figure 2B). Interestingly, the number of CUG⁺/Pax7⁺ account for 29% at baseline and 23% post

training of the total positive CUG nuclei (Figure 2B). These results show that satellite cells possess that CUG mutation, despite being mitotically inactive, and can have implications towards dysregulation.

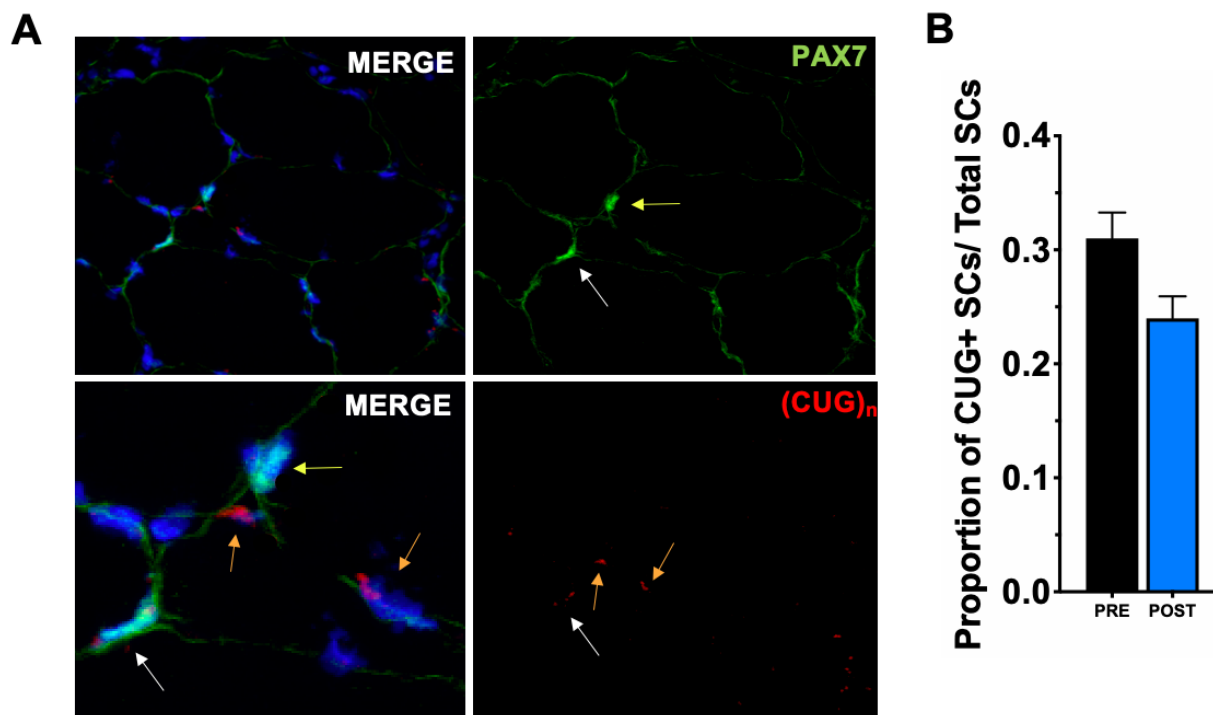


Figure 2. SCs in DM1 possess CUG nuclear foci accumulation.

(A) Representative image of combination fluorescent *in situ* hybridization probing for CUG repeats with immunohistochemical staining of SCs in DM1 skeletal muscle. (B) Quantification of CUG⁺/PAX7⁺/DAPI⁺ as a percentage of total PAX7⁺.

Next, we examined factors of muscle quality that have been implicated in SC dysfunction and are present in multiple muscle-wasting diseases. The quantification of muscle capillaries was performed on 25 type 1 and 25 type 2 muscles per subject, per time point⁹⁷. Our results show a type 2 specific lower CFPE (0.80- folds relative to CTRL) and capillaries per fibre (C/Fi)(0.70- folds relative to CTRL), that is alleviated following training (1.33- fold increase relative to PRE in CFPE, 1.56- folds increase relative to PRE in C/Fi) ($p < 0.05$, Figure 3B, C). The capillary density did not significantly differ between groups (Figure 3D).

With regards to threshold analysis of BODIPY and perilipin staining, both show no differences between groups (Figure 3F, G). However, upon closer inspection of muscle samples, we observed the presence of highly atrophic (i.e., markedly reduced CSA), fat infiltrated muscle fibres (Figure 1H). These fibres had an extremely high signal of BODIPY that was not present in adjacent fibres and showed signs of adiposity as exhibited by large “holes” representative of fat vacuoles.

We sought to investigate fibrosis in DM1 skeletal muscle with Masson’s trichrome staining, which stain collagen blue⁹⁸. We show a staggering 52.7- and 43.4- fold increase in collagen accumulation in DM1 Pre- and Post- training muscle, respectively compared to the CTRL ($p < 0.05$, Figure 3I). Taken together, our results confirm that DM1 muscle exhibits markers of poor muscle quality, and therefore disturbances in the SC niche that could perturb SC function.

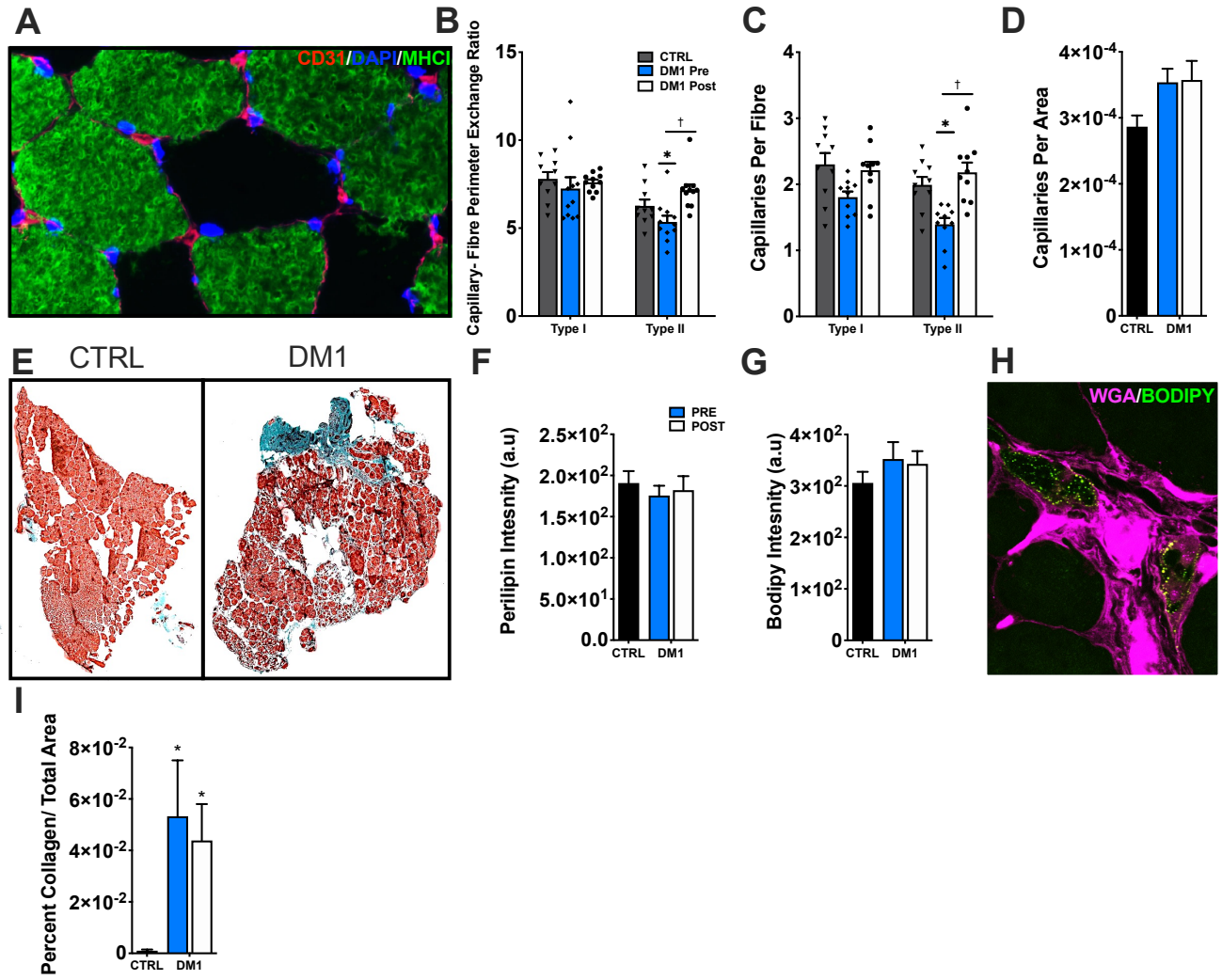


Figure 3. DM1 muscle has markers of poor muscle quality.

(A) Representative stain of CD31/MHC1/LAMININ/DAPI in healthy muscle (B) characterization of CFPE or a measure of the number of capillaries per fibre, sharing factor of the capillaries, relative to the individual fibres' perimeter. (C) Quantification of capillaries per fibre-type. (D) Overall capillary density relative to the total area of quantification. (E) Representative Masson's trichrome stain of age-matched CTRL and DM1 muscle sections. (F, G) Threshold analysis of Bodipy and perilipin signal,

respectively. (H) Representative image of hyper-positive fat infiltrated muscle fibres only present in DM1 tissue. (I) quantification of Mason's trichrome stain via threshold analysis of sections for collagen. Values represent means \pm SEM; * $P < 0.05$ significant DM1 vs CTRL, obtained through one-way ANOVA with a Fisher LSD post-hoc test; † $P < 0.05$ significant DM1 PRE vs POST using a paired t-test ($n = 11$ per group).

To gain insight on the mechanisms regarding SC dysfunction in DM1, we performed proliferation assays on DM1 patient myoblasts *in vitro*. BrdU actively incorporates into dividing cells following S-phase⁹⁹, and MTT assay which labels viable cells during proliferation events and can be used as a marker for activation¹⁰⁰. MTT assays show that DM1 myoblasts have a proliferation defect as they display 2.50- fold less viable cells than passage-matched CTRL cells ($p < 0.05$, Figure 4B).

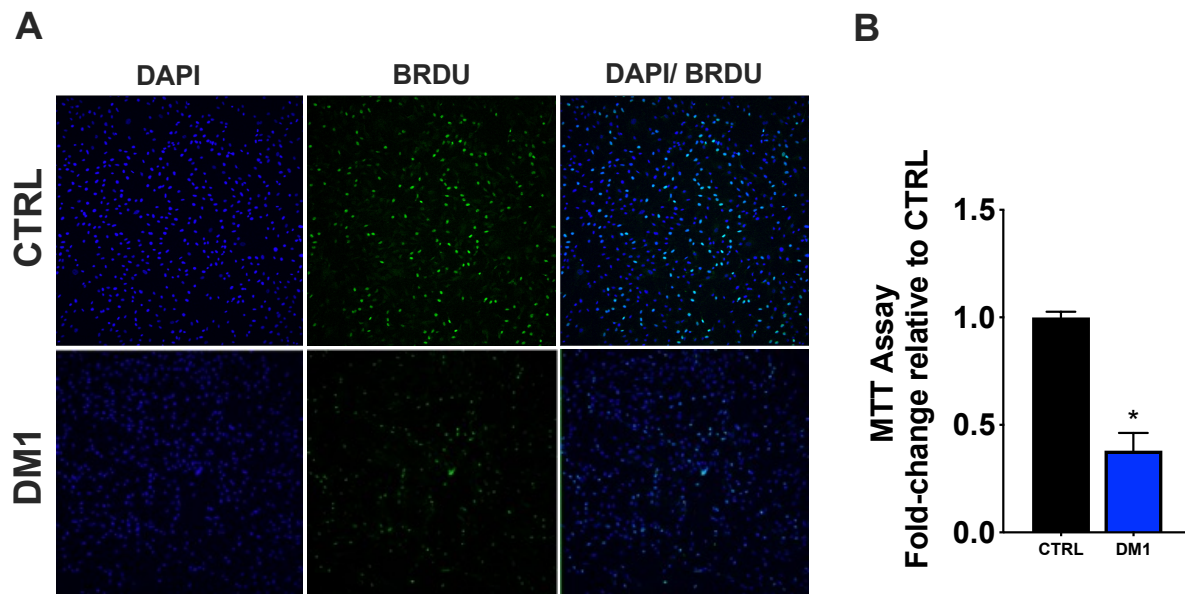


Figure 4. *DM1 patient myoblasts have a proliferation defect.*

(A) Representative 10x image of primary myoblasts co-stained with DAPI and BRDU, which labels S-phase or proliferating myoblasts. (B) Fold-change quantification of MTT colorimetric assay relative to CTRL. Values represent means \pm SEM; * $P < 0.05$ significant with an unpaired Student's t-test ($n=2$ CTRL, $n=3$ DM1). Experiments were performed in quadruplicate

We sought to better characterize metabolic disturbances in both DM1 myoblasts and myotubes as a potential mechanism underpinning the observed myogenic defect. In myoblasts our results indicate an impairment in multiple aspects of mitochondrial respiration. We show a 2.70-fold lower basal respiration, 2.05-fold lower maximal respiratory capacity, a 2.48-fold lower proton leak and a 2.75-fold lower ATP production in DM1 myoblasts compared to CTRL ($p < 0.05$, Figure 5B). We observe no significant differences in spare respiratory capacity, non-mitochondrial O₂ consumption and coupling efficiency (Figure 5B). Interestingly, metabolic perturbances were completely normalized in oxygen consumption rates of DM1 Day-6 myotubes, where no metabolic outcomes were significantly differed from the CTRL (Figure 5E).

The dynamics between utilizing glycolysis versus oxidative phosphorylation as the primary source of metabolism has implications towards the myogenic program. Our results indicate lower ECAR in DM1 myoblasts. More specifically, we show a 2.23-fold lower glycolysis, 2.83-fold lower glycolytic capacity, and a 4.16-fold lower glycolytic reserve ($p < 0.05$, Figure 5E). We show no significant differences in non-glycolysis acidification between groups (Figure 5E). These results indicate severe impairments in mitochondrial respiration and glycolysis in DM1 myoblasts, that may not persist in terminally differentiated states.

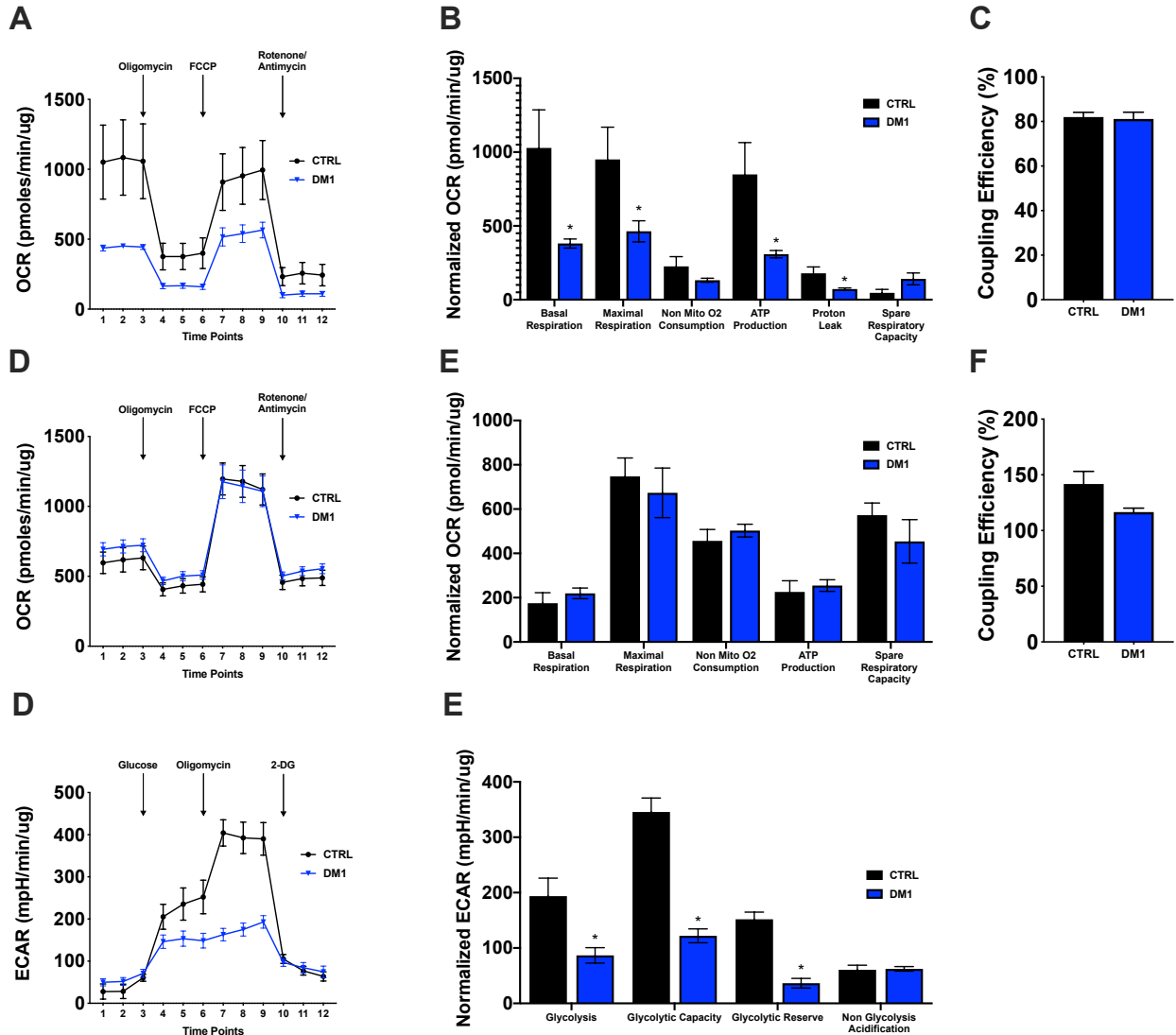


Figure 5. DM1 myoblasts display decreased respiratory capacity and glycolysis, oxygen consumption normalized in myotubes.

(A) Kinetic OCR response normalized to protein content in DM1 and CTRL myoblasts obtained through Seahorse XFe24 MitoStress Test. (B,C) Quantification of individual mitochondrial respiratory functions and coupling efficiencies in DM1 and CTRL lines.(D) Representation of kinetic OCR normalized to protein content in DM1 versus control in day-6 myotubes. (E) Quantification of individual measures obtained from OCR curve efficiencies in DM1 and CTRL myotubes. (F) Coupling efficiency of myotubes. (G)

Kinetic ECAR curves of DM1 and CTRL myoblasts normalized to protein content. (G)
Glycolytic parameters obtained from ECAR kinetic curve of DM1 and CTRL myoblasts.
Values represent means \pm SEM, * $P < 0.05$ using an unpaired Student's t-test (n=2, per group).

Discussion

In the present study we show a significantly elevated SC pool in both fibre types in DM1 skeletal muscle, with the type-2 specific SCs further increasing following aerobic training. We show no differences at baseline with activation status between DM1 and control, although an increase in nuclei per myofiber area and myogenin protein content suggest greater differentiation and fusion. As expected, we also show greater fibrosis and fat infiltration in DM1 skeletal muscle vs control, indicative of poor muscle quality. For the first time, we show a lower type-2 muscle capillarization, that is completely rescued following training, emphasizing a therapeutic potential of exercise in DM1. Our *in vitro* results also confirm a proliferation defect in DM1. Finally, we show a decreased mitochondrial respiration and glycolysis in DM1 patient myoblasts, with mitochondrial respiration normalizing to the control values in myotubes.

Elevated SC pool in DM1

In the present study we show that DM1 skeletal muscle has 2.24- and 1.84- fold higher type 1 and type 2 associated SCs, respectively, compared to healthy controls. Satellite cells are dysregulated in a number of muscular dystrophies such BMD, CMD, muscle-eye-brain disease, FSHD, OPMD, EDMD and sarcoglycanopathies, with an elevated SC pool having also been reported in DMD^{101,102,103}. Elevated SC pool with progressive muscle atrophy is indicative of a dysregulation of SCs, as SCs typically would protect against degeneration. This latter is evidenced

by the fewer SCs observed with atrophy due to muscle damage and aging associated sarcopenia. In muscular dystrophies however, the presence of a genetic mutation central to muscle maintenance leads to both direct and indirect effects that can cause SC abnormalities. Direct effects include a mutation in genes that perturb SC function and are present in SCs.

A notable indirect effect is observed in DMD, caused by the loss of dystrophin due to a mutation on the *DMD* gene, that results in a larger SC pool as a compensation for a hostile muscle environment. Dystrophin is required for muscle structure and integrity of skeletal muscle, and the subsequent loss of dystrophin leads to the chronic cycling of SCs to initiate regeneration to combat the ongoing degeneration of the skeletal muscle¹⁰⁴. Ultimately, this causes SCs to continuously activate and thereby enter the cell cycle leading to cellular exhaustion or senescence¹⁰⁵. This is evidenced by significantly reduced telomere length in DMD SCs compared to healthy controls¹⁰⁵. Interestingly, DM1 SCs exhibit premature senescence without telomere shortening^{47,88}, indicating that SCs are not excessively cycling. The latter finding implies that the SC dysfunction in DM1 could be a direct effect of the CUG mutation underscoring dysfunction. Moreover, in the present study we show a total of 1.62% of eMHC positive fibres at baseline similar to previous studies⁴⁴, indicative of functional regeneration, which is much lower than the staggering 40% observed in DMD^{45,106}. These results further emphasize that ongoing regeneration cannot solely explain SC dysfunction and therefore an intrinsic defect is the most plausible hypothesis. Our FISH data shows that approximately 30% of SCs possess CUG nuclear foci, in line with previous studies⁶⁸, indicating that the mutation is present in SCs and therefore could affect SC function. Other *in vitro* studies display that the induction of CUG triplet repeat expansion in myoblasts lead to phenotypic abnormalities in differentiation in otherwise healthy myoblasts⁵⁹. Furthermore, genetic correction of the CUG repeat expansion, significantly increased proliferation of SCs⁴⁸. This implies a direct

causal link between the CUG mutation and the SC function that dominate the SC ability to orchestrate regeneration.

Interestingly, in the present study our *in vivo* results show no differences in MyoD evaluated by both immunohistochemistry and western blotting, but an increase in myogenin protein. MyoD is both a signal of SC activation and activates the downstream target myogenin for differentiation. Multiple *in vitro* studies suggest that MyoD is impaired in DM1 and accounts for the differentiation defect^{59,89}. These studies suggest abnormally low MyoD protein levels occur due to the hyperphosphorylation of CUGBP1, are suboptimal to activate myogenin and therefore impair differentiation. However, upstream signalling of MyoD and downstream of myogenin signalling of myogenin are intact in DM1, suggesting that the binding of MyoD to myogenin is impaired⁵⁹. In healthy skeletal muscle, activation of SCs result in an upregulation of both MyoD and Myf5, and commitment is represented by a downregulation of Pax7, Myf5 while MyoD remains elevated to activate myogenin¹⁰⁷. Therefore, heterodimerization of MyoD to E-box factors to induce myogenin is suggested to be dysregulated in DM1 and can explain the normal levels observed in the present study. This is the first study to our knowledge, to quantify MyoD and myogenin in DM1 human biopsies. In the present study, patient biopsies were taken at rest conditions, therefore do not encapsulate activation capacity of satellite cells. Under a stress response such as eccentric damage, MyoD activation peaks at 48- hours following the response however at basal conditions MyoD+/Pax7+ SCs represent “snapshot” activation and are therefore present in very small quantities¹⁰⁸. Therefore, future studies should aim to characterize MyoD following a stress response, such as eccentric damage to quantify whether there is an impairment in activation in DM1 in response to physiological stimuli.

A significant increase of myogenin protein paired with a trending decrease in the type 1 myonuclear domain may suggest that SCs in DM1 are driven towards differentiation and myogenin-dependent fusion *in vivo*. The presence of eMHC fibres and centrally located nuclei indicate regeneration is present in DM1, therefore the upregulation of myogenin can also signify an increased regeneration as SCs are driven towards fusion to facilitate an increase in the myonuclear domain and increase muscle protein synthesis to combat atrophy. A study by Vatemmi and colleagues (2004) showed that sarcoplasmic masses, or areas of myofibrillar dysregulation, which are widely present in DM1 show an activation of differentiation markers desmin, NCAM, bcl-2, IGF-1 and p57, although they did not reach complete maturation¹⁰⁹. The use of whole muscle homogenates, and thereby inclusion of sarcoplasmic masses in western blotting could account for the upregulation of myogenin in DM1.

In line with literature, our *in vitro* results show a reduction in proliferation in DM1 myoblasts^{51,69,88,110}. Genetic editing to lessen the number of CUG repeats significantly improved the proliferation defect but still remained significantly impaired from the control⁴⁸. This result suggests that the intrinsic defects of the CUG repeat expansion in myoblasts plays a role in a proliferation defect; however, other factors are involved. Furthermore, MBNL1 overexpression through adenoviral transfection improved proliferation capacity, but remained lower than the control⁴⁸. This suggested that the sequestration⁴⁸ of MBNL1 also plays a role in the proliferation defect. The role of MBNL family proteins in muscle health is well characterized, and research suggests that compound loss of MBNL1 and MBNL2 is responsible for the muscular phenotype in DM1¹¹¹. Research also shows that MBNL1 plays a role in healthy muscle development. During postnatal skeletal muscle development relocates from the cytoplasm back to the nucleus to orchestrate several alternative splicing events that are involved in contraction, sarcomere structure

and signalling and healthy formation of skeletal muscle⁹⁴. In DM1, MBNL1 is both sequestered in the nucleus and misspliced meaning it is unable to perform its splicing functions to adequately facilitate muscle development⁹⁴. Another study has suggested that the missplicing of MBNL1 and MBNL2 occurs early myogenesis and persist into myotube formation¹¹². Therefore, it is unsurprising that MBNL protein sequestration and missplicing add to the myogenic defects in DM1.

DM1 SCs are responsive to exercise

A promising finding in the present study is the further increase of the SC pool following 12 weeks of aerobic training. Skeletal muscle is a highly plastic tissue that can adapt to various stimuli including different modes of exercise. With aerobic training, muscle adapts through increases in capillarization, mitochondrial biogenesis, a shift towards a more oxidative phenotype. Several studies indicate a role of SCs mediated remodelling in the absence of hypertrophy, indicating that SCs can regulate muscle plasticity with aerobic training¹¹³. For example, 6 weeks of aerobic training in sedentary women resulted in an increase in the number of Pax7+ cells and MyoD/Pax7+ cells associated with hybrid fibres, or muscle fibres expressing both type 1 and type 2 myosin heavy chain¹¹⁴. The presence of SC increases in hybrid fibres suggest the role of SCs in remodeling of type 2 to type 1 skeletal muscle fibres due to aerobic training.

In the present study unpublished data from Mikhail and colleagues, suggest that aerobic training in DM1 lead to a trending increase of type 1 muscle fibres ($p=0.06$) and non-statistically significant increase in type 2 muscle fibre ($p=0.1$) cross sectional area. Furthermore, aerobic training resulted in a 1.6 kg increase in lean mass of DM1 patients. Taken together, these results suggest that aerobic training intensity of 70% max work output for these patients lead to muscle

hypertrophy and therefore was not a true aerobic stimulus. These results can explain the further increase in the type-2 associated SCs observed in the present study to facilitate muscle hypertrophy. The increase of SC content and CSA following training is well documented in literature and is required to achieve substantial muscle hypertrophy. SCs facilitate muscle hypertrophy through the donation of a nuclei to the parental fibre, thereby increasing the muscle protein synthesis capabilities, and enabling the muscle to grow. The typical SC response to training observed in DM1 patients, indicated that these cells respond normally to exercise and therefore exercise possesses therapeutic potential. Whether SC expansion through proliferation results in SCs that carry less of the mutational load remains to be elucidated and is an important question constituting further enhancements in the pool.

Full Rescue of Muscle Capillarization in DM1- implications towards SCs

Skeletal muscle perfusion is critical for maintaining muscle health as it provides muscle with oxygen, growth factors while carrying away waste products such as carbon dioxide. In the present study we show that as baseline DM1 skeletal muscle has lower type 2 muscle capillarization vs healthy controls. Revascularization is a vital part of muscle regeneration, and inadequate perfusion can add to regeneration deficit observed in DM1³⁴. There is a spatiotemporal relationship between capillaries and SCs in humans, emphasizing the importance of adequate vascularization on SC function¹¹⁵. Both activated and differentiated SCs are located in close proximity to capillaries, the latter being associated with neoangiogenesis¹¹⁵. This can be further evidenced by VEGF, primary factor in angiogenesis, overexpression promoting myotube formation and hypertrophy, and inhibition resulting in hypotrophy¹¹⁶. Furthermore, individuals with higher baseline muscle capillarization results in a greater expansion of the SC pool and activated SCs following eccentric

damage¹¹⁷. Furthermore, 24 weeks of resistance training resulted in a significant elevation in satellite cell content, and type 2 muscle CSA in elderly individuals with high baseline capillarization, with no significant improvements observed in individuals with low muscle capillarization¹¹⁸. Taken together, these results suggest that muscle capillarization is a critical factor in SC function. SCs being in close proximity to capillaries result in a faster diffusion rate, and a thereby greater exposure to a number of myokines known to modulate SC activity. This includes myostatin, hepatocyte growth factor, insulin-like growth factor 1, VEGF and IL-6. Following ischemic injury in mice, combined administration of VEGF and IGF1 lead to both angiogenesis and SC proliferation and subsequent functional regeneration of skeletal muscle¹¹⁹.

A known potent stimulator of muscle capillarization is aerobic training. Consistent with this finding, our results show a complete rescue of muscle vascularization in type 2 skeletal muscles following aerobic training. An increase in muscle capillarization enables SCs to better respond to anabolic stimuli, thereby potentially improving function. Improvements in systemic signalling and environment has been shown through parabiosis experiments to improve functionality and regenerative capacity of old SCs when exposed to a young environment^{120,121}. This exemplifies the retained ability for SCs to respond to systemic signalling and improve function. What remains to be elucidated in DM1 literature is whether systemic signalling of myokines is impaired in DM1 and if improvements in capillarization would better modulate SC behaviour. Nonetheless, the complete rescue of capillarization following aerobic training has implications towards improved muscle quality and regeneration.

Skeletal muscle 'quality' improved after exercise

In the present study we show that DM1 skeletal muscle displays approximately a 50-fold greater amount of fibrosis relative to control. Fibrosis in DM1 has been reported in both skeletal and cardiac muscle previously⁴²¹²². Induction of CUG repeats in mice resulted in a missplicing of multiple extracellular matrix genes such as collagen, elastin, as well as formation and regulation of collagen matrix¹²³. These results were independent of MBNL1 sequestration, indicating that the CUG repeat expansion intrinsically causes dysregulation of ECM components.

Excessive collagen accumulation has implications towards SC function as it leads to disturbances in the niche. The niche, or the microenvironment of the SC cell, is defined by the borders of the basal lamina and sarcolemma of the muscle fibre. SC behaviour is regulated in part by the niche through delivery of systemic and paracrine signalling as well as establishing polarity that dictates SC fate³⁷¹²⁴. In fact, elderly individuals show type 2 associated SC encapsulated by excessive laminin thickness, consistent with a type-2 specific decline observed with age¹²⁵. These SCs were less likely to become activated indicating that excessive fibrosis inhibits SC proliferation¹²⁵. In both aging and DMD, dysfunctional SCs tend to become pro-fibrogenic due to alterations in systemic signalling leading to the activation of Wnt signalling pathways, causing these cells to contribute to the accumulation of fibrosis¹²⁰¹²⁶. Therefore, dysfunctionality in SCs can further contribute to the fibrosis observed in DM1. Ultimately, increased fibrosis observed in DM1 has implications for both decreased muscle health as well as impaired SC function.

Impaired mitochondrial respiration in DM1 myoblasts, normalization with differentiation

In the present study we are the first, to our knowledge, to investigate mitochondrial respiration in DM1 myoblasts. Our results show a defect in mitochondrial respiration and glycolysis in DM1 myoblasts, where oxidative phosphorylation is restored to control levels in

myotubes. Garcia-Puga and colleagues (2020) showed a similar impairment in mitochondrial respiration in patient derived myoblasts with decreases in basal respiration, max respiration, ATP production; however, they did not show any differences in glycolysis³³.

The orchestration of anaerobic and aerobic metabolism has implications towards dictating SC fate. During quiescence and differentiation, SCs rely predominantly on OXPHOS as the main energy source, whereas during proliferation SCs rely on glycolysis⁷⁷. The reduction in glycolytic capacity in myoblasts could in part explain proliferation defects observed *in vitro* in DM1. Stem cells have mechanisms to actively repress OXPHOS in favour of glycolysis during proliferation, this includes activation of Hif1a, PDK and the downregulation of ETC complex III, IV and V⁷⁴. Hif1a knockout delayed injury induced muscle repair due to the reduction of proliferation and drive towards differentiation through inhibition of Notch signalling, a key mediator in SC stemness¹²⁷. This suggests that proper glycolysis represents a key factor in proper proliferation signalling in SC function. The complete normalization of mitochondrial respiration during differentiation, along with *in vivo* data suggesting an upregulation of differentiation markers suggest that terminal differentiation in DM1 satellite cells may not be impaired. Instead, the notion of the metabolic “switch” that occurs between glycolysis and OXPHOS to signal differentiation being impaired in DM1 warrants further investigation. MBNL1-null C2C12 resulted in decreased PGC1a expression, a marker of mitochondrial biogenesis and lower membrane potential¹²⁸. Song and colleagues (2020) also noted that MBNL1 overexpression resulted in a partial rescue of the proliferation defect in DM1 myoblasts⁴⁸. Taken together these results suggest the MBNL1 sequestration in DM1 may underscore the mitochondrial impairments that lead to SC dysfunction in DM1.

In DMD, SCs have distinct metabolic perturbations displaying fewer mitochondria, less ATP production and reduced oxygen consumption rates, where SC dysfunction is also observed¹²⁹. This emphasizes that mitochondrial impairments may contribute to the dysfunction. In fact, transplantation of endurance trained SCs into *mdx* mice resulted in improvements in mitochondrial biogenesis and restoration of oxygen consumption rates¹³⁰. Furthermore, 4 weeks of aerobic training in healthy mice protected against SC cycling through suppression of Akt-mTOR pathway producing a limited activation status of SCs, potentially explaining beneficial effects of exercise in DMD SCs¹³¹. Interestingly, *MBLN1* overexpression was shown to ameliorate the proliferation defect in DM1 SCs through an mTOR upregulation⁴⁸. This suggests that potentially an optimal mTOR threshold is required to maintain SC integrity, where DMD may result in overexpression leading to excessive activation and DM1 may result in decreased activation through suboptimal mTOR expression. Nonetheless, this research provides compelling evidence of the therapeutic avenue that aerobic training can elicit on the metabolic profile of satellite cells, and thereby function. Aerobic training, a potent stimulus of mitochondrial biogenesis, in old wild-type mice resulted in improved regeneration as noted by increased cross sectional area, decreased number of centrally located nuclei and greater satellite cell following cardiotoxin injection compared to untrained counterpart¹³². Furthermore, aerobic training can improve SC function through the increase in SC self-renewal or proliferation markers, and enhanced myogenic colony formation through the inhibition of mitochondrial respiration¹³³. This further emphasizes the abilities for aerobic training to overcome the proliferation defect in DM1 SCs and override the drive towards differentiation.

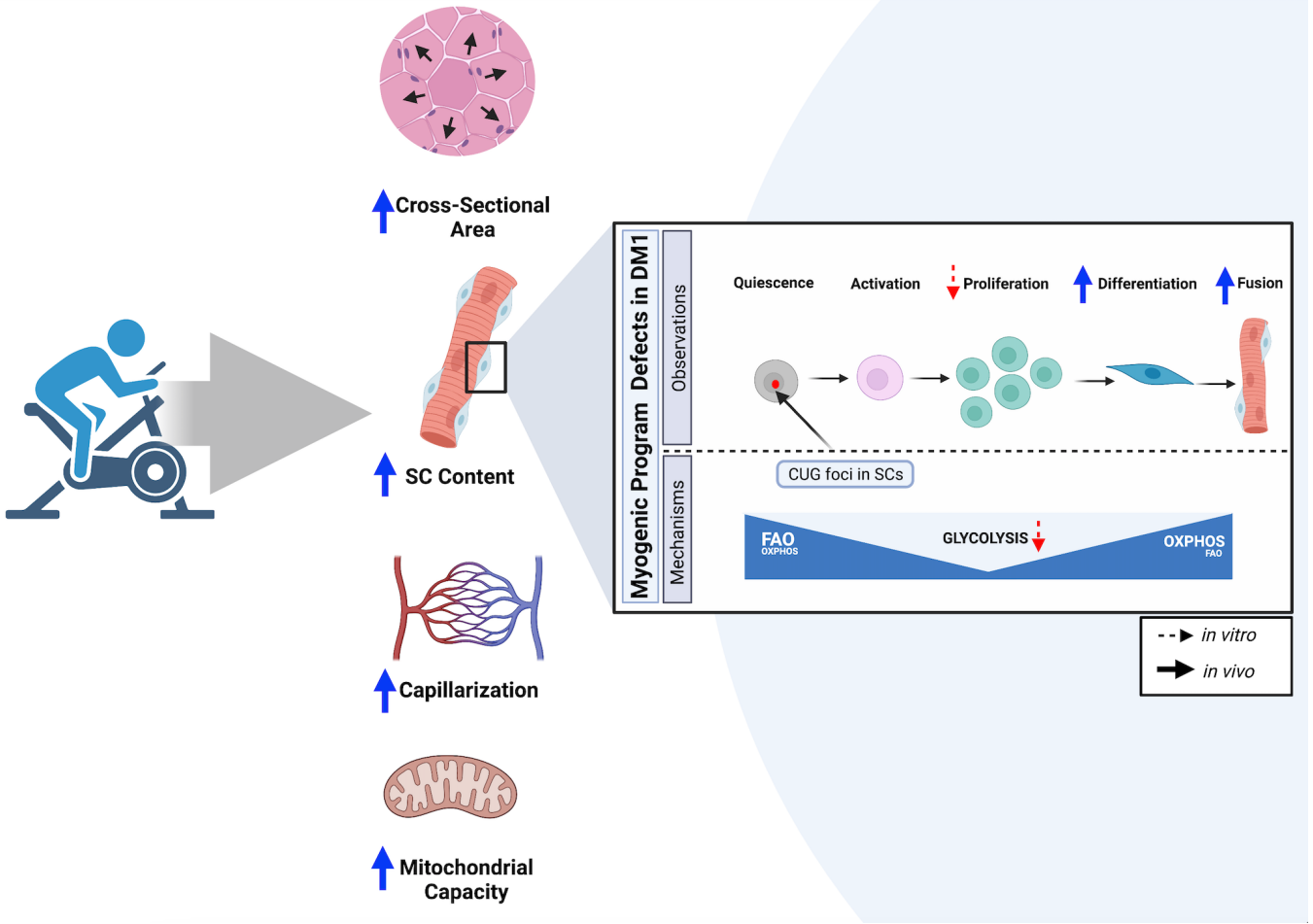


Figure 1. Summary of the results

Conclusion

In the present study, we show that DM1 skeletal muscle has a significantly elevated SC pool that remains responsive to exercise. We show that DM1 muscle shows signs of ongoing regeneration evidenced through the presence of eMHC fibres. Our data indicates that SCs possess the CUG triplet repeat expansion, most likely underscoring myogenic defects observed. These include dysregulations of the myogenic program with decreased proliferation *in vitro* and a drive towards differentiation *in vivo*. Furthermore, impairments in SC cell function are further evidenced by poor muscle quality such as decreased muscle capillarization, increased fibrosis and fat infiltration, despite the elevation in SC pool. We show that aerobic training fully rescues the muscle

capillarization defect, implicating a responsiveness of DM1 skeletal muscle to aerobic training, that increases quality of skeletal muscle. Finally, our results suggest that metabolic disturbances in myoblasts may contribute to myogenic program dysfunction, as both glycolysis and mitochondrial respiration is impaired in myoblasts, with normalization in myotubes. Taken together, along with unpublished data from our lab, we suggest a therapeutic potential of aerobic training on muscle health and potentially modulating improvements in SC function. Future studies should aim to better elucidate whether further SC expansion in DM1 results in expansion of the mutation, or if these cells give rise to better daughter cells more protected against the mutation. Moreover, whether CUG positive SCs are fundamentally different than the CUG negative counterparts. Furthermore, greater emphasis should be made in literature on DM1 being both a stem cell disorder and metabolic disorder to further research in the field.

Limitations and Future Directions

Some limitations in our study are that the *in vitro* samples were not obtained from the same individuals participating in the exercise trial. This is a limitation because both the repeats and the age differ, and these factors both can affect the proliferation, differentiation and mitochondrial results obtained. Due to COVID-19 restrictions on human research we were not able to recruit more controls and therefore purchased control cell lines from Lonza, with a limited inventory. Furthermore, another limitation is using myoblasts versus primary satellite cells. Myoblasts are activated SCs expressing MRFs, and therefore quiescent measures cannot be studied. Future studies should examine whether the inability to maintain quiescence results in myogenic defects. Another limitation of the present study is that MyoD⁺/Pax7⁺ cells were quantified using PRE and POST biopsies, where the post was taken a minimum of three days after the last training session. This means that's without sequential biopsies following an acute

bout of exercise or an eccentric damage protocol we cannot gain insight on whether activation of SCs is impaired *in vivo*. Given the population of DM1 patients, we would not have considered taking sequential biopsies or subjecting them to an eccentric damage protocol to limit patient discomfort in the study. Other future directions would include an *in vitro* experiment to mimic exercise in these cells such as electrical pulse stimulation. This would enable research on mechanistic benefits of exercise on DM1 myoblasts, and parallel our exercise trial study.

References

1. Chau, A. & Kalsotra, A. Developmental insights into the pathology of and therapeutic strategies for DM1: Back to the basics. *Dev. Dyn.* **244**, 377–390 (2015).
2. Bird, T. D. Myotonic Dystrophy Type 1. *GeneReviews®* (2021).
3. Thornton, C. A. Myotonic dystrophy. *Neurologic Clinics* vol. 32 705–719 (2014).
4. Yotova, V. *et al.* Anatomy of a founder effect: myotonic dystrophy in Northeastern Quebec. doi:10.1007/s00439-005.
5. Johnson, N. E. *et al.* Population-Based Prevalence of Myotonic Dystrophy Type 1 Using Genetic Analysis of Statewide Blood Screening Program. *Neurology* **96**, e1045–e1053 (2021).
6. Brook, J. D. *et al.* Molecular basis of myotonic dystrophy: Expansion of a trinucleotide (CTG) repeat at the 3' end of a transcript encoding a protein kinase family member. *Cell* **68**, 799–808 (1992).
7. De Temmerman, N. *et al.* Intergenerational Instability of the Expanded CTG Repeat in the DMPK Gene: Studies in Human Gametes and Preimplantation Embryos. *Am. J. Hum. Genet.* **75**, 325–329 (2004).
8. Redman, J. B., Fenwick, R. G., Fu, Y.-H., Pizzuti, A. & Caskey, C. T. Relationship Between Parental Trinucleotide GCT Repeat Length and Severity of Myotonic Dystrophy in Offspring. *JAMA* **269**, 1960–1965 (1993).
9. Tsilfidis, C., MacKenzie, A. E., Mettler, G., Barceló, J. & Korneluk, R. G. Correlation between CTG trinucleotide repeat length and frequency of severe congenital myotonic dystrophy. *Nat. Genet.* **1992** *13* **1**, 192–195 (1992).
10. Barceló, J. M., Mahadevan, M. S., Tsilfidis, C., MacKenzie, A. E. & Korneluk, R. G. Intergenerational stability of the myotonic dystrophy protomutation. *Hum. Mol. Genet.* **2**, 705–709 (1993).
11. Martorell, L., Monckton, D. G., Sanchez, A., Munain, A. L. de & Baiget, M. Frequency and stability of the myotonic dystrophy type 1 premutation. *Neurology* **56**, 328–335 (2001).
12. Beaton, L. J., Tarnopolsky, M. A. & Phillips, S. M. Variability in Estimating Eccentric Contraction-Induced Muscle Damage and Inflammation in Humans. *Can. J. Appl. Physiol.* **27**, 516–526 (2002).
13. MC, Ø., P, A.-S., M, D., JM, H. & J, V. Endocrine function in 97 patients with myotonic dystrophy type 1. *J. Neurol.* **259**, 912–920 (2012).
14. André, L. M., Ausems, C. R. M., Wansink, D. G. & Wieringa, B. Abnormalities in skeletal muscle myogenesis, growth, and regeneration in myotonic dystrophy. *Frontiers in Neurology* vol. 9 368 (2018).
15. Davis, B. M., McCurrach, M. E., Taneja, K. L., Singer, R. H. & Housman, D. E. Expansion of a CUG trinucleotide repeat in the 3' untranslated region of myotonic dystrophy protein kinase transcripts results in nuclear retention of transcripts. *Proc. Natl. Acad. Sci.* **94**, 7388–7393 (1997).
16. Taneja, K. L., McCurrach, M., Schalling, M., Housman, D. & Singer, R. H. Foci of trinucleotide repeat transcripts in nuclei of myotonic dystrophy cells and tissues. *J. Cell Biol.* **128**, 995–1002 (1995).
17. Napierala, M. & Krzyzosiak, W. J. CUG Repeats Present in Myotonin Kinase RNA Form Metastable “Slippery” Hairpins *. *J. Biol. Chem.* **272**, 31079–31085 (1997).
18. Miller, J. W. *et al.* Recruitment of human muscleblind proteins to (CUG)_n expansions

- associated with myotonic dystrophy. *EMBO J.* **19**, 4439–4448 (2000).
19. Wang, E. T. *et al.* Transcriptome-wide Regulation of Pre-mRNA Splicing and mRNA Localization by Muscleblind Proteins. *Cell* **150**, 710–724 (2012).
 20. Mankodi, A. *et al.* Expanded CUG Repeats Trigger Aberrant Splicing of ClC-1 Chloride Channel Pre-mRNA and Hyperexcitability of Skeletal Muscle in Myotonic Dystrophy. *Mol. Cell* **10**, 35–44 (2002).
 21. Savkur, R. S., Philips, A. V. & Cooper, T. A. Aberrant regulation of insulin receptor alternative splicing is associated with insulin resistance in myotonic dystrophy. *Nat. Genet.* **29**, 40–47 (2001).
 22. Fugier, C. *et al.* Misregulated alternative splicing of BIN1 is associated with T tubule alterations and muscle weakness in myotonic dystrophy. *Nat. Med.* **17**, 720–725 (2011).
 23. Thornton, C. A. Myotonic Dystrophy. *Neurol. Clin.* **32**, 705–719 (2014).
 24. Tang, Z. Z. *et al.* Muscle weakness in myotonic dystrophy associated with misregulated splicing and altered gating of CaV1.1 calcium channel. *Hum. Mol. Genet.* **21**, 1312–1324 (2012).
 25. Hardie, D. G., Ross, F. A. & Hawley, S. A. AMPK: a nutrient and energy sensor that maintains energy homeostasis. *Nat. Rev. Mol. Cell Biol.* **13**, 251–262 (2012).
 26. Brockhoff, M. *et al.* Targeting deregulated AMPK/mTORC1 pathways improves muscle function in myotonic dystrophy type I. *J. Clin. Invest.* **127**, 549–563 (2017).
 27. Ravel-Chapuis, A., Al-Rewashdy, A., Bélanger, G. & Jasmin, B. J. Pharmacological and physiological activation of AMPK improves the spliceopathy in DM1 mouse muscles. *Hum. Mol. Genet.* **27**, 3361–3376 (2018).
 28. Manta, A. *et al.* Chronic exercise mitigates disease mechanisms and improves muscle function in myotonic dystrophy type 1 mice. *J. Physiol.* **597**, 1361–1381 (2019).
 29. Aldehag, A. *et al.* Effects of hand-training in persons with myotonic dystrophy type 1 – a randomised controlled cross-over pilot study. <https://doi.org/10.3109/09638288.2012.754952> **35**, 1798–1807 (2013).
 30. Kierkegaard, M. & Tollbäck, A. Reliability and feasibility of the six minute walk test in subjects with myotonic dystrophy. *Neuromuscul. Disord.* **17**, 943–949 (2007).
 31. Brady, L. I., MacNeil, L. G. & Tarnopolsky, M. A. Impact of habitual exercise on the strength of individuals with myotonic dystrophy type 1. *Am. J. Phys. Med. Rehabil.* **93**, (2014).
 32. Siciliano, G. *et al.* Coenzyme Q10, exercise lactate and CTG trinucleotide expansion in myotonic dystrophy. *Brain Res. Bull.* **56**, 405–410 (2001).
 33. García-Puga, M., Saenz-Antoñanzas, A., Fernández-Torrón, R., Munain, A. L. de & Matheu, A. Myotonic Dystrophy type 1 cells display impaired metabolism and mitochondrial dysfunction that are reversed by metformin. *Aging (Albany, NY)*. **12**, 6260–6275 (2020).
 34. S, B.-F. Skeletal muscle regeneration after injury: an overview. *J. Voice* **8**, 53–62 (1994).
 35. Jaiswal, N. *et al.* The role of skeletal muscle Akt in the regulation of muscle mass and glucose homeostasis. *Mol. Metab.* **28**, 1 (2019).
 36. MAURO, A. Satellite cell of skeletal muscle fibers. *J. Biophys. Biochem. Cytol.* **9**, 493–495 (1961).
 37. Yin, H., Price, F. & Rudnicki, M. A. Satellite cells and the muscle stem cell niche. *Physiol. Rev.* **93**, 23–67 (2013).

38. Murach, K. A. *et al.* Starring or Supporting Role? Satellite Cells and Skeletal Muscle Fiber Size Regulation. <https://doi.org/10.1152/physiol.00019.2017> **33**, 26–38 (2017).
39. Seale, P. *et al.* Pax7 is required for the specification of myogenic satellite cells. *Cell* **102**, 777–786 (2000).
40. Vihola, A. *et al.* Histopathological differences of myotonic dystrophy type 1 (DM1) and PROMM/DM2. *Neurology* **60**, 1854–1857 (2003).
41. Thomas, J. D., Oliveira, R., Sznajder, Ł. J. & Swanson, M. S. Myotonic Dystrophy and Developmental Regulation of RNA Processing. *Compr. Physiol.* **8**, 509–553 (2018).
42. Ozimski, L. L., Sabater-Arcis, M., Bargiela, A. & Artero, R. The hallmarks of myotonic dystrophy type 1 muscle dysfunction. *Biol. Rev.* **96**, 716–730 (2021).
43. Thornton, C. A., Johnson, K. & Moxley, R. T. Myotonic dystrophy patients have larger CTG expansions in skeletal muscle than in leukocytes. *Ann. Neurol.* **35**, 104–107 (1994).
44. Thornell, L.-E. *et al.* Satellite cell dysfunction contributes to the progressive muscle atrophy in myotonic dystrophy type 1. *Neuropathol. Appl. Neurobiol.* **35**, 603–613 (2009).
45. Decary, S. *et al.* Shorter telomeres in dystrophic muscle consistent with extensive regeneration in young children. *Neuromuscul. Disord.* **10**, 113–120 (2000).
46. Wang, Y. *et al.* Abnormal nuclear aggregation and myotube degeneration in myotonic dystrophy type 1. *Neurol. Sci.* 2019 406 **40**, 1255–1265 (2019).
47. Thornell, L.-E. *et al.* Satellite cell dysfunction contributes to the progressive muscle atrophy in myotonic dystrophy type 1. *Neuropathol. Appl. Neurobiol.* **35**, 603–613 (2009).
48. Song, K. Y. *et al.* MBNL1 reverses the proliferation defect of skeletal muscle satellite cells in myotonic dystrophy type 1 by inhibiting autophagy via the mTOR pathway. *Cell Death Dis.* **11**, 1–16 (2020).
49. Furling, D. *et al.* Defective satellite cells in congenital myotonic dystrophy. *Hum. Mol. Genet.* **10**, 2079–2087 (2001).
50. Bigot, A. *et al.* Large CTG repeats trigger p16-dependent premature senescence in myotonic dystrophy type 1 muscle precursor cells. *Am. J. Pathol.* **174**, 1435–1442 (2009).
51. Renna, L. V. *et al.* Premature Senescence in Primary Muscle Cultures of Myotonic Dystrophy Type 2 is not Associated with p16 Induction. *Eur. J. Histochem.* **58**, 275–286 (2014).
52. Gao, Y. *et al.* Genome Therapy of Myotonic Dystrophy Type 1 iPS Cells for Development of Autologous Stem Cell Therapy. *Mol. Ther.* **24**, 1378–1387 (2016).
53. Loro, E. *et al.* Normal myogenesis and increased apoptosis in myotonic dystrophy type-1 muscle cells. *Cell Death Differ.* **17**, 1315–1324 (2010).
54. Beffy, P. *et al.* Altered signal transduction pathways and induction of autophagy in human myotonic dystrophy type 1 myoblasts. *Int. J. Biochem. Cell Biol.* **42**, 1973–1983 (2010).
55. Kaur, J. & Debnath, J. Autophagy at the crossroads of catabolism and anabolism. *Nat. Rev. Mol. Cell Biol.* 2015 168 **16**, 461–472 (2015).
56. Wu, S.-Y., Lan, S.-H. & Liu, H.-S. Degradative autophagy selectively regulates CCND1 (cyclin D1) and MIR224, two oncogenic factors involved in hepatocellular carcinoma tumorigenesis. <https://doi.org/10.1080/15548627.2019.1569918> **15**, 729–730 (2019).
57. Fortini, P. *et al.* The fine tuning of metabolism, autophagy and differentiation during in vitro myogenesis. *Cell Death Dis.* 2016 73 **7**, e2168–e2168 (2016).
58. Kim, J., Kundu, M., Viollet, B. & Guan, K.-L. AMPK and mTOR regulate autophagy through direct phosphorylation of Ulk1. *Nat. Cell Biol.* 2011 132 **13**, 132–141 (2011).
59. Amack, J. D., Reagan, S. R. & Mahadevan, M. S. Mutant DMPK 3'-UTR transcripts

- disrupt C2C12 myogenic differentiation by compromising MyoD. *J. Cell Biol.* **159**, 419 (2002).
60. LA, S., A, G.-G., P, S., A, A. & MA, R. Reduced differentiation potential of primary MyoD^{-/-} myogenic cells derived from adult skeletal muscle. *J. Cell Biol.* **144**, 631–643 (1999).
 61. DA, B. *et al.* Promoter-specific regulation of MyoD binding and signal transduction cooperate to pattern gene expression. *Mol. Cell* **9**, 587–600 (2002).
 62. Segalés, J., Perdiguero, E. & Muñoz-Cánoves, P. Regulation of Muscle Stem Cell Functions: A Focus on the p38 MAPK Signaling Pathway. *Front. Cell Dev. Biol.* **0**, 91 (2016).
 63. Timchenko, N. A. *et al.* Overexpression of CUG Triplet Repeat-binding Protein, CUGBP1, in Mice Inhibits Myogenesis. *J. Biol. Chem.* **279**, 13129–13139 (2004).
 64. Salisbury, E. *et al.* Ectopic expression of cyclin D3 corrects differentiation of DM1 myoblasts through activation of RNA CUG-binding protein, CUGBP1. *Exp. Cell Res.* **314**, 2266–2278 (2008).
 65. Salisbury, E. *et al.* Ectopic expression of cyclin D3 corrects differentiation of DM1 myoblasts through activation of RNA CUG-binding protein, CUGBP1. *Exp. Cell Res.* **314**, 2266–2278 (2008).
 66. Jones, K. *et al.* GSK3 β mediates muscle pathology in myotonic dystrophy. *J. Clin. Invest.* **122**, 4461–4472 (2012).
 67. Peng, X. *et al.* Celf1 regulates cell cycle and is partially responsible for defective myoblast differentiation in myotonic dystrophy RNA toxicity. *Biochim. Biophys. Acta - Mol. Basis Dis.* **1852**, 1490–1497 (2015).
 68. Yadava, R. S. *et al.* Modeling muscle regeneration in RNA toxicity mice. *Hum. Mol. Genet.* **30**, 1111–1130 (2021).
 69. Furling, D. *et al.* Defective satellite cells in congenital myotonic dystrophy. *Hum. Mol. Genet.* **10**, 2079–2087 (2001).
 70. Gladman, J. T. *et al.* NKX2-5, a modifier of skeletal muscle pathology due to RNA toxicity. *Hum. Mol. Genet.* **24**, 251 (2015).
 71. Loro, E. *et al.* Normal myogenesis and increased apoptosis in myotonic dystrophy type-1 muscle cells. *Cell Death Differ.* **17**, 1315–1324 (2010).
 72. Relaix, F. *et al.* Perspectives on skeletal muscle stem cells. *Nat. Commun.* **2021 121 12**, 1–11 (2021).
 73. Khacho, M. *et al.* Mitochondrial Dynamics Impacts Stem Cell Identity and Fate Decisions by Regulating a Nuclear Transcriptional Program. *Cell Stem Cell* **19**, 232–247 (2016).
 74. Khacho, M. & Slack, R. S. Mitochondrial activity in the regulation of stem cell self-renewal and differentiation. *Curr. Opin. Cell Biol.* **49**, 1–8 (2017).
 75. Ryall, J. G., Cliff, T., Dalton, S. & Sartorelli, V. Metabolic Reprogramming of Stem Cell Epigenetics. *Cell Stem Cell* **17**, 651–662 (2015).
 76. Rocheteau, P., Gayraud-Morel, B., Siegl-Cachedenier, I., Blasco, M. A. & Tajbakhsh, S. A Subpopulation of Adult Skeletal Muscle Stem Cells Retains All Template DNA Strands after Cell Division. *Cell* **148**, 112–125 (2012).
 77. Bhattacharya, D. & Scimè, A. Mitochondrial Function in Muscle Stem Cell Fates. *Front. Cell Dev. Biol.* **0**, 480 (2020).
 78. Liberti, M. V. & Locasale, J. W. The Warburg Effect: How Does it Benefit Cancer Cells? *Trends Biochem. Sci.* **41**, 211 (2016).

79. Theret, M. *et al.* AMPK α 1-LDH pathway regulates muscle stem cell self-renewal by controlling metabolic homeostasis. *EMBO J.* **36**, 1946–1962 (2017).
80. Ryall, J. G. *et al.* The NAD⁺-Dependent SIRT1 Deacetylase Translates a Metabolic Switch into Regulatory Epigenetics in Skeletal Muscle Stem Cells. *Cell Stem Cell* **16**, 171–183 (2015).
81. Pala, F. *et al.* Distinct metabolic states govern skeletal muscle stem cell fates during prenatal and postnatal myogenesis. *J. Cell Sci.* **131**, (2018).
82. Shintaku, J. *et al.* MyoD Regulates Skeletal Muscle Oxidative Metabolism Cooperatively with Alternative NF- κ B. *Cell Rep.* **17**, 514–526 (2016).
83. Moore, T. M. *et al.* Mitochondrial Dysfunction Is an Early Consequence of Partial or Complete Dystrophin Loss in mdx Mice. *Front. Physiol.* **0**, 690 (2020).
84. Motohashi, N. & Asakura, A. Muscle satellite cell heterogeneity and self-renewal. *Front. Cell Dev. Biol.* **0**, 1 (2014).
85. Onopiuk, M. *et al.* Mutation in dystrophin-encoding gene affects energy metabolism in mouse myoblasts. *Biochem. Biophys. Res. Commun.* **386**, 463–466 (2009).
86. Matre, P. R. *et al.* CRISPR/Cas9-Based Dystrophin Restoration Reveals a Novel Role for Dystrophin in Bioenergetics and Stress Resistance of Muscle Progenitors. *Stem Cells* **37**, 1615–1628 (2019).
87. Yin, H., Price, F. & Rudnicki, M. A. Satellite Cells and the Muscle Stem Cell Niche. <https://doi.org/10.1152/physrev.00043.2011> **93**, 23–67 (2013).
88. Bigot, A. *et al.* Large CTG Repeats Trigger p16-Dependent Premature Senescence in Myotonic Dystrophy Type 1 Muscle Precursor Cells. *Am. J. Pathol.* **174**, 1435–1442 (2009).
89. Timchenko, N. A. *et al.* Overexpression of CUG Triplet Repeat-binding Protein, CUGBP1, in Mice Inhibits Myogenesis *. *J. Biol. Chem.* **279**, 13129–13139 (2004).
90. Wang, M. *et al.* Correction of Glycogen Synthase Kinase 3 β in Myotonic Dystrophy 1 Reduces the Mutant RNA and Improves Postnatal Survival of DMSXL Mice. *Mol. Cell Biol.* **39**, (2019).
91. MA, T., E, P., K, S. & B, L. Suction-modified Bergström muscle biopsy technique: experience with 13,500 procedures. *Muscle Nerve* **43**, 716–725 (2011).
92. Mackey, A. L. *et al.* Assessment of satellite cell number and activity status in human skeletal muscle biopsies. *Muscle Nerve* **40**, 455–465 (2009).
93. Hepple, R. T., Mackinnon, S. L. M., Goodman, J. M., Thomas, S. G. & Plyley, M. J. Resistance and aerobic training in older men: effects on V_o 2 peak and the capillary supply to skeletal muscle. <https://doi.org/10.1152/jappl.1997.82.4.1305> **82**, 1305–1310 (1997).
94. Lin, X. *et al.* Failure of MBNL1-dependent post-natal splicing transitions in myotonic dystrophy. *Hum. Mol. Genet.* **15**, 2087–2097 (2006).
95. Wheeler, T. M. *et al.* Reversal of RNA Dominance by Displacement of Protein Sequestered on Triplet Repeat RNA. *Science (80-.).* **325**, 336–339 (2009).
96. Nakamori, M., Pearson, C. E. & Thornton, C. A. Bidirectional transcription stimulates expansion and contraction of expanded (CTG) \cdot (CAG) repeats. *Hum. Mol. Genet.* **20**, 580–588 (2011).
97. Porter, M. M., Koolage, C. W. & Lexell, J. Biopsy sampling requirements for the estimation of muscle capillarization. *Muscle Nerve* **26**, 546–548 (2002).
98. Goldner, J. A modification of the masson trichrome technique for routine laboratory

- purposes. *Am. J. Pathol.* **14**, 237 (1938).
99. C, L., J, H., G, D., N, A. & JP, T. In vitro bromodeoxyuridine labeling of nuclei: application to myotube hybridization. *J. Histochem. Cytochem.* **39**, 1421–1426 (1991).
 100. Gerlier, D. & Thomasset, N. Use of MTT colorimetric assay to measure cell activation. *J. Immunol. Methods* **94**, 57–63 (1986).
 101. Morgan, J. E. & Zammit, P. S. Direct effects of the pathogenic mutation on satellite cell function in muscular dystrophy. *Exp. Cell Res.* **316**, 3100–3108 (2010).
 102. Ishimoto, S., Goto, I., Ohta, M. & Kuroiwa, Y. A quantitative study of the muscle satellite cells in various neuromuscular disorders. *J. Neurol. Sci.* **62**, 303–314 (1983).
 103. Maier, F. & Bornemann, A. COMPARISON OF THE MUSCLE FIBER DIAMETER AND SATELLITE CELL FREQUENCY IN HUMAN MUSCLE BIOPSIES. (1999) doi:10.1002/(SICI)1097-4598(199905)22:5.
 104. Blau, H. M., Webster, C. & Pavlath, G. K. Defective myoblasts identified in Duchenne muscular dystrophy. *Proc. Natl. Acad. Sci.* **80**, 4856–4860 (1983).
 105. Sacco, A. *et al.* Short Telomeres and Stem Cell Exhaustion Model Duchenne Muscular Dystrophy in mdx/mTR Mice. *Cell* **143**, 1059–1071 (2010).
 106. Webster, C., Silberstein, L., Hays, A. P. & Blau, H. M. Fast muscle fibers are preferentially affected in Duchenne muscular dystrophy. *Cell* **52**, 503–513 (1988).
 107. Dumont, N. A., Wang, Y. X. & Rudnicki, M. A. Intrinsic and extrinsic mechanisms regulating satellite cell function. *Development* **142**, 1572–1581 (2015).
 108. Snijders, T. *et al.* Satellite cells in human skeletal muscle plasticity. *Frontiers in Physiology* vol. 6 283 (2015).
 109. Vattermi, G. *et al.* Expression of late myogenic differentiation markers in sarcoplasmic masses of patients with myotonic dystrophy. *Neuropathol. Appl. Neurobiol.* **31**, 45–52 (2005).
 110. Song, N. *et al.* Overexpression of platelet-derived growth factor-BB increases tumor pericyte content via stromal-derived factor-1 α /CXCR4 axis. *Cancer Res.* **69**, 6057–6064 (2009).
 111. KY, L. *et al.* Compound loss of muscleblind-like function in myotonic dystrophy. *EMBO Mol. Med.* **5**, 1887–1900 (2013).
 112. André, L. M., Cruchten, R. T. P. van, Willemse, M. & Wansink, D. G. (CTG) n repeat-mediated dysregulation of MBNL1 and MBNL2 expression during myogenesis in DM1 occurs already at the myoblast stage. *PLoS One* **14**, e0217317 (2019).
 113. Joannis, S., Snijders, T., Nederveen, J. P. & Parise, G. The Impact of Aerobic Exercise on the Muscle Stem Cell Response. *Exerc. Sport Sci. Rev.* **46**, 180–187 (2018).
 114. Joannis, S. *et al.* Evidence for the contribution of muscle stem cells to nonhypertrophic skeletal muscle remodeling in humans. *FASEB J.* **27**, 4596–4605 (2013).
 115. Christov, C. *et al.* Muscle Satellite Cells and Endothelial Cells: Close Neighbors and Privileged Partners. <https://doi.org/10.1091/mbc.e06-08-0693> **18**, 1397–1409 (2007).
 116. BA, B. *et al.* Coordinated vascular endothelial growth factor expression and signaling during skeletal myogenic differentiation. *Mol. Biol. Cell* **19**, 994–1006 (2008).
 117. Nederveen, J. P. *et al.* The influence of capillarization on satellite cell pool expansion and activation following exercise-induced muscle damage in healthy young men. *J. Physiol.* **596**, 1063–1078 (2018).
 118. Snijders, T. *et al.* Muscle fibre capillarization is a critical factor in muscle fibre hypertrophy during resistance exercise training in older men. *J. Cachexia. Sarcopenia*

- Muscle* **8**, 267–276 (2017).
119. Borselli, C. *et al.* Functional muscle regeneration with combined delivery of angiogenesis and myogenesis factors. *Proc. Natl. Acad. Sci.* **107**, 3287–3292 (2010).
 120. AS, B. *et al.* Increased Wnt signaling during aging alters muscle stem cell fate and increases fibrosis. *Science* **317**, 807–810 (2007).
 121. IM, C. *et al.* Rejuvenation of aged progenitor cells by exposure to a young systemic environment. *Nature* **433**, 760–764 (2005).
 122. Petri, H. *et al.* Myocardial fibrosis in patients with myotonic dystrophy type 1: a cardiovascular magnetic resonance study. *J. Cardiovasc. Magn. Reson.* **16**, 59 (2014).
 123. Du, H. *et al.* Aberrant alternative splicing and extracellular matrix gene expression in mouse models of myotonic dystrophy. *Nat. Struct. Mol. Biol.* **17**, 187 (2010).
 124. Thomas, K., Engler, A. J. & Meyer, G. A. Extracellular matrix regulation in the muscle satellite cell niche. <https://doi.org/10.3109/03008207.2014.947369> **56**, 1–8 (2014).
 125. Nederveen, J. P. *et al.* Age-related changes to the satellite cell niche are associated with reduced activation following exercise. *FASEB J.* **34**, 8975–8989 (2020).
 126. Biressi, S., Miyabara, E. H., Gopinath, S. D., Carlig, P. M. M. & Rando, T. A. A Wnt-TGF β 2 axis induces a fibrogenic program in muscle stem cells from dystrophic mice. *Sci. Transl. Med.* **6**, 267ra176–267ra176 (2014).
 127. Yang, X., Yang, S., Wang, C. & Kuang, S. The hypoxia-inducible factors HIF1 α and HIF2 α are dispensable for embryonic muscle development but essential for postnatal muscle regeneration. *J. Biol. Chem.* **292**, 5981–5991 (2017).
 128. Yokoyama, S. *et al.* MBNL1-Associated Mitochondrial Dysfunction and Apoptosis in C2C12 Myotubes and Mouse Skeletal Muscle. *Int. J. Mol. Sci.* **2020**, Vol. 21, Page 6376 **21**, 6376 (2020).
 129. Bell, E. L. *et al.* PPAR δ modulation rescues mitochondrial fatty acid oxidation defects in the mdx model of muscular dystrophy. *Mitochondrion* **46**, 51–58 (2019).
 130. Mohiuddin, M. *et al.* Transplantation of Muscle Stem Cell Mitochondria Rejuvenates the Bioenergetic Function of Dystrophic Muscle. *bioRxiv* 2020.04.17.017822 (2020) doi:10.1101/2020.04.17.017822.
 131. Chen, Z. *et al.* Exercise protects proliferative muscle satellite cells against exhaustion via the Igfbp7-Akt-mTOR axis. *Theranostics* **10**, 6448 (2020).
 132. Joannis, S. *et al.* Exercise conditioning in old mice improves skeletal muscle regeneration. *FASEB J.* **30**, 3256–3268 (2016).
 133. Abreu, P. & Kowaltowski, A. J. Satellite cell self-renewal in endurance exercise is mediated by inhibition of mitochondrial oxygen consumption. *J. Cachexia. Sarcopenia Muscle* **11**, 1661–1676 (2020).